

Electron-phonon interactions and lattice dynamics of optic phonons in semiconductor heterostructures

K. J. Nash

*Defence Research Agency (RSRE), St. Andrews Road, Great Malvern,
Worcestershire, WR14 3PS, United Kingdom*

(Received 10 December 1991; revised manuscript received 8 June 1992)

Slab vibrations, reformulated slab vibrations, and guided vibrations have been proposed by various authors as the confined polar-optic-phonon modes in heterostructures. It is shown, with reference to these three cases, that both the intrasubband and intersubband electron-phonon scattering rates are independent of the basis set used to describe the phonon modes, as long as this set is orthogonal and complete. Earlier conflicting results are attributed to the use of basis sets that do not satisfy these criteria, and to scattering potentials that do not obey the correct boundary conditions. Nearly all the scattering is by modes that are well described by continuum models. A dispersive continuum theory of the lattice dynamics is developed. Without recourse to microscopic theory, we derive the connection rules that relate fields on either side of an interface, and identify the circumstances in which each above-mentioned set of vibrations corresponds to the normal modes. The controversy over whether the normal modes satisfy electromagnetic or mechanical boundary conditions is resolved. The design of lattice properties to minimize electron-phonon scattering rates is discussed.

I. INTRODUCTION

The scattering of electrons by polar-optic phonons governs a number of important properties of semiconductor heterostructures, including room-temperature carrier mobilities,¹ hot-electron relaxation rates,² intersubband transition rates,^{3,4} and room-temperature exciton lifetimes.⁵⁻⁷ Although microscopic calculations of the normal modes of heterostructures are now a well-established technique,⁸ calculations of electron-phonon scattering generally adopt a continuum treatment of the lattice dynamics, in order to reduce the complexity of the problem. Since the discovery⁹ that the confined longitudinal-optic (LO) modes of a slab do not have the form predicted in the usual treatment of the dielectric continuum model (DCM),¹⁰ a number of different continuum models of the modes have been used to calculate electron-phonon-scattering rates,¹¹⁻¹⁶ and not all of these have given the same results. Different vibrational basis sets, called slab vibrations, reformulated slab vibrations, and guided vibrations, have been considered¹¹⁻¹³ as possible normal modes. The main purpose of this paper is to reconcile the conflicting results by making a detailed study of the different models and pointing out where errors have been made.

In addition, the continuum mechanics of optic modes in polar heterostructures is discussed. It is shown that several problems can be resolved, including the issue of the boundary conditions (BC's) that are obeyed by the optic modes,^{9,13,17,18} without recourse to microscopic theories.

The rest of this paper is organized as follows. The different vibrational basis sets are investigated in Sec. II, in particular the question of whether they are orthogonal and complete. Section III calculates the electron-phonon interactions for each basis set, and in Sec. IV these results

are applied to the calculation of scattering rates. Section V compares the results with those of previous work. In Secs. II-V, the different vibrational basis sets are treated on an equal footing and the question of which, if any, corresponds to the normal modes is not addressed. This question is addressed in Sec. VI, which gives a detailed account of the continuum mechanics of optic modes in polar heterostructures. Finally, the conclusions of this work and the consequences for phonon band-structure engineering are discussed in Sec. VII.

II. OPTIC-PHONON VIBRATIONS

The first step in investigating whether a set of vibrations can be used as a basis set for the normal modes is to ask whether the set is orthogonal and complete. Now, in the continuum theory of the mechanics of the optic modes, the dynamical fields are $\Phi(\mathbf{r})$, the electrostatic potential, and $\mathbf{w}(\mathbf{r}) = \rho^{1/2}\mathbf{u}(\mathbf{r})$, where $\mathbf{u}(\mathbf{r})$ is the displacement from equilibrium of the positive ions less that of the negative ions, and ρ is the reduced mass per unit volume of the lattice. Electromagnetic retardation and the coupling to the ionic center-of-mass vibrations, which at small wave vector represent the acoustic modes, are ignored. The kinetic-energy density is $\frac{1}{2}|\dot{\mathbf{w}}|^2$, and the orthogonality relation for the normal modes or for a vibrational basis set is thus

$$\int d^3\mathbf{r} \mathbf{w}_\mu^*(\mathbf{r}) \cdot \mathbf{w}_\nu(\mathbf{r}) = 0, \quad \mu \neq \nu. \quad (1)$$

We consider a heterostructure composed of a series of layers of different binary semiconductors (the generalization to ternaries^{19,20} is straightforward but is omitted for the sake of simplicity). We are concerned with the vibrations that are confined to the layer $0 < z < d$, i.e., with $\mathbf{w}(\mathbf{r}) = 0$ beyond this layer. The layer has a mirror plane

at $z = d/2$, and we choose vibrational basis functions that are symmetric or antisymmetric with respect to reflection in this mirror. For the polar-optic vibrations, $\mathbf{w}(\mathbf{r})$ can be written for $0 < z < d$ as the gradient of a mechanical scalar potential,

$$\mathbf{w} = -\nabla\bar{\chi}, \quad (2)$$

but $\mathbf{w}(\mathbf{r})$ may be discontinuous and not obey Eq. (2) at $z = 0$ and d . When in addition there is translational invariance in the x - y plane so that $\bar{\chi}(\mathbf{r}) = \chi(z)\exp(i\mathbf{q}\cdot\boldsymbol{\rho})$, where $\boldsymbol{\rho} = (x, y)$, then vibrations with different \mathbf{q} are orthogonal. For vibrations with the same \mathbf{q} the orthogonality relation (1) becomes

$$\chi_\mu^* \cdot \chi_\nu = 0, \quad \mu \neq \nu, \quad (3)$$

where this dot product for mechanical potentials $\chi_\nu(z)$ is defined by

$$\chi_\mu^* \cdot \chi_\nu = \frac{1}{2d} \int_0^d dz q^2 \chi_\mu^*(z) \chi_\nu(z) + \frac{d\chi_\mu^*}{dz} \frac{d\chi_\nu}{dz}. \quad (4)$$

The label ν identifies different members of a vibrational basis set, which may or may not correspond to the normal modes. ν comprises the in-plane wave vector \mathbf{q} and an integer n . n distinguishes the vibrations for which \mathbf{q} is the same (when the vibrations correspond to the normal modes this means that n labels the different phonon branches). The completeness condition for the normal modes or for any vibrational basis set $\chi_{n\mathbf{q}}(z)\exp(i\mathbf{q}\cdot\boldsymbol{\rho})$ is that, for each \mathbf{q} and for an arbitrary function $\psi(z)$,

$$\lim_{m \rightarrow \infty} \Delta_m^* \cdot \Delta_m = 0, \quad (5)$$

where

$$\Delta_m \equiv \psi(z) - \sum_{n=0}^m c_n \chi_{n\mathbf{q}}(z) \quad (6)$$

and

$$c_n = \frac{\chi_{n\mathbf{q}}^* \cdot \psi}{\chi_{n\mathbf{q}}^* \cdot \chi_{n\mathbf{q}}}, \quad (7)$$

and the dot product is that defined by Eq. (4). When this completeness condition is satisfied, any vibration can be represented as a linear combination of the basis functions $\chi_{n\mathbf{q}}(z)\exp(i\mathbf{q}\cdot\boldsymbol{\rho})$.

Before describing the different sets of polar-optic vibrations that have been proposed as normal modes, it is useful to define "interface vibrations" and "bulklike vibrations" and say how these are related to the normal modes in a dispersionless continuum model.¹⁰ The interface vibrations obey $\nabla^2\bar{\chi} = 0$ and thus comprise the set $\chi = \chi_{\bar{2}\mathbf{q}}(z) = \cosh q(z - d/2)$, $\chi = \chi_{\bar{1}\mathbf{q}}(z) = \sinh q(z - d/2)$ (i.e., labeled $n = \bar{2}$ and $\bar{1}$, respectively). The bulklike vibrations are orthogonal to the interface vibrations, the conditions thereby imposed on the bulklike potential being

$$\chi_\nu(0) = \chi_\nu(d) = 0. \quad (8)$$

Any $\chi(z)$ that obeys these conditions represents a bulklike vibration. The normal modes of a heterostructure are straightforward if the dispersion of the LO phonons in the bulk semiconductors is neglected.¹⁰ The bulklike vibrations of a layer are degenerate normal modes at the LO phonon frequency ω_L ; the other normal modes are interface modes,¹⁰ which are formed from linear combinations of interface vibrations in the different layers.

The sets of vibrations whose properties will be discussed, the slab vibrations, reformulated slab vibrations, and guided vibrations, are listed in Table I. The slab vibrations have $\chi_{n\mathbf{q}} = 0$ at the interfaces, and are identical to the bulklike modes that arise in the conventional treatment of the DCM.¹⁰ The reformulated slab vibrations are a refinement⁷ of a set of vibrations proposed by Huang and Zhu¹¹ and are defined to obey $\chi_{n\mathbf{q}} = \chi'_{n\mathbf{q}} = 0$ at the interfaces, since under certain circumstances (Sec. VI B) this leads to agreement with the modes found in microscopic calculations. The reformulated slab vibrations are⁷

$$\chi_{n\mathbf{q}}(z') = \cos(\mu_{n\mathbf{q}}\pi z'/d) + D_{n\mathbf{q}} \cosh qz', \quad n = 0, 2, 4, \dots, \quad (9a)$$

TABLE I. Sets of functions that describe the polar-optic vibrations of a semiconductor slab extending from $z = 0$ to d . Column 2 gives the mechanical potential $\chi_{n\mathbf{q}}(z)$ for the vibrations, with $n = 0, 1, 2, \dots$. Symmetric vibrations have even n , and antisymmetric vibrations have odd n . The $\chi_{n\mathbf{q}}(z)$ are solutions of Eq. (10) with the boundary conditions (BC's) at $z = 0$ and d given in column 3. Each set of vibrations is complete for functions $\psi(z)$ that obey the BC's at $z = 0$ and d given in column 4. The BC $\psi = 0$ can be removed by including the interface vibrations (IV's) in the set (column 5). Column 6 gives the expression for $-\beta V_{n\mathbf{q}}(z)$ for $0 \leq z \leq d$, where $\bar{V}_{n\mathbf{q}}(\mathbf{r}) = V_{n\mathbf{q}}(z)\exp(i\mathbf{q}\cdot\boldsymbol{\rho})$ is the electrostatic potential that occurs in the Hamiltonian (11) for the electron-phonon interaction.

Name of vibrations	$\chi_{n\mathbf{q}}(z)$	$\chi_{n\mathbf{q}}$ obeys BC's	BC's for complete set	For a complete set without BC's	$-\beta V_{n\mathbf{q}}(z)$
Slab set	$\sin \frac{(n+1)\pi z}{d}$	$\chi_{n\mathbf{q}} = \chi'_{n\mathbf{q}} = 0$	$\psi = 0$	Include IV's	$\chi_{n\mathbf{q}}(z)$
Reformulated slab set	Eq. (9)	$\chi_{n\mathbf{q}} = \chi'_{n\mathbf{q}} = 0$	$\psi = 0$	Include IV's	$\chi_{n\mathbf{q}}(z)$
Guided set	$\cos \frac{n\pi z}{d}$	$\chi'_{n\mathbf{q}} = \chi'''_{n\mathbf{q}} = 0$	No restrictions	No additional vibrations required	Eq. (14)
Interface vibrations	$\left\{ \begin{array}{l} \cosh q(z - d/2) \\ \sinh q(z - d/2) \end{array} \right.$				$\exp(-qd/2)\sinh(qd/2)\chi_{n\mathbf{q}}(z)$ $\exp(-qd/2)\cosh(qd/2)\chi_{n\mathbf{q}}(z)$

$$\chi_{nq}(z') = \sin(\mu_{nq}\pi z'/d) + D_{nq} \sinh qz', \quad (9b)$$

where $z' = z - d/2$, and D_{nq} and μ_{nq} are chosen, with $n+1 < \mu_{nq} \leq n+2$, so that χ_{nq} and its derivative both vanish at $z' = \pm d/2$. The derivation of the reformulated slab vibrations from the DCM is discussed in Refs. 11 and 7. (The difference between the reformulated slab vibrations of Eq. (9) and those of Ref. 11 is discussed in Sec. V.) The slab and reformulated slab sets both satisfy Eq. (8), and so give alternative descriptions of the bulklike vibrations. The guided vibrations are defined to obey $\chi'_{nq} = 0$ at the interfaces so that they agree with the $q=0$ modes observed in Raman backscattering.⁹ They do not obey (8), and so they are linear combinations of the bulklike and interface vibrations.

The simplest way to generate complete orthogonal sets of functions is as the eigenfunctions of a suitable differential equation. For the present work, a suitable equation (see Appendix A) is the fourth-order eigenvalue equation

$$\left[\frac{d^2}{dz^2} + k_{nq}^2 \right] \left[\frac{d^2}{dz^2} - q^2 \right] \chi_{nq}(z) = 0. \quad (10)$$

k_{nq}^2 is the eigenvalue and $k_{nq}z$ is the argument of the sinusoidal terms of χ_{nq} . The "standard boundary conditions" (SBC's), i.e., the BC's for which the differential operators in this equation are Hermitian, are discussed in Appendix A, where they are given by Eq. (A4). Each set of basis functions in Table I obeys Eq. (10) and SBC's at $z=0$ and d . The particular boundary conditions that χ_{nq} obeys in order to satisfy SBC's are given for each set in the third column of Table I. The orthogonality and completeness of each set can be demonstrated for these boundary conditions by using the same methods as for second-order Sturm-Liouville equations (Appendix A). The boundary conditions on the functions $\psi(z)$ for which each set is complete can be relaxed from those given in the third column of Table I to those of the fourth column (Appendix B). When the boundary condition $\psi=0$ remains, it can be removed by including the interface vibrations in the set (column five of Table I). This is because [with the two interface vibrations labeled $n=\bar{1}$ and $\bar{2}$ as above, and c_n defined by Eq. (7)] the function $\psi - c_{\bar{1}}\chi_{\bar{1}q} - c_{\bar{2}}\chi_{\bar{2}q}$ is orthogonal to the interface vibrations and thus vanishes at $z=0$ and d .

In summary, each of the following three sets of vibrations has been shown to be orthogonal and complete: the slab and interface vibrations together; the reformulated slab and interface vibrations together; and the guided vibrations. We can further conclude that the interface and bulklike vibrations together form a complete set. The differential equation (10) was selected purely because of its suitability for proving these results. However, it will be shown in Sec. VI that Eq. (10) can in fact be derived from the equations of motion for optic modes, and that the sets of vibrations discussed here correspond in some circumstances to normal modes. Sets that are orthogonal and complete are related by unitary transformations. For the complete sets of vibrations discussed here, the unitary transformations are presented in Appendix C.

III. ELECTRON-PHONON INTERACTIONS

The electron-phonon interactions for the different sets of vibrations can be deduced from their mechanical potentials $\chi_{nq}(z)$. The polar-optic vibrations, which are the subject of this paper, are the ones that have a macroscopic electrostatic potential and therefore scatter electrons strongly, with electron-phonon interaction Hamiltonian

$$H_{ep}(\mathbf{r}) = -e \sum_{\nu} \bar{V}_{\nu}(\mathbf{r}) \left[\frac{2\omega_{\nu}}{\hbar} \right]^{1/2} Q_{\nu}, \quad (11)$$

where Q_{ν} and ω_{ν} are the normal coordinate and angular frequency, respectively, for the mode ν , and $-e$ is the electron charge. The quantity $\bar{V}_{\nu}(\mathbf{r})$ is equal to the electrostatic potential $\Phi_{\nu}(\mathbf{r})$ when the lattice displacement is given by

$$(2\omega_{\nu}/\hbar)^{1/2} Q_{\nu} = 1. \quad (12)$$

Thus $\bar{V}_{\nu}(\mathbf{r})$ obeys Poisson's equation

$$\frac{-1}{\epsilon(\infty)} \nabla \cdot [\epsilon(z; \infty) \nabla \bar{V}_{\nu}] = \frac{1}{\beta} \left[\nabla^2 \bar{\chi}_{\nu} - \frac{\partial \bar{\chi}_{\nu}}{\partial z} \Big|_{z=d} \delta(z-d+\eta) + \frac{\partial \bar{\chi}_{\nu}}{\partial z} \Big|_{z=0} \delta(z-\eta) \right], \quad (13)$$

with boundary conditions $\bar{V}_{\nu} \bar{V}'_{\nu} = 0$ at $z = \pm \infty$. $\epsilon(z; \infty)$ is the high-frequency dielectric constant as a function of z , and $\epsilon(\infty)$ is its value for $0 < z < d$. η is a positive infinitesimal. β is given by

$$\beta^{-1} = \frac{\hbar\omega_L}{e} \left[\frac{2\pi r_p \alpha}{\Omega d I_{\nu}} \right]^{1/2},$$

where ω_L is the LO phonon frequency, r_p is the polaron radius, α is the Fröhlich coupling parameter, I_{ν} is the norm $\chi_{\nu}^* \cdot \chi_{\nu}$ given by Eq. (4) [the presence of which expresses the normalization condition (12)], and Ω is the area of the structure in the x - y plane. $\bar{\chi}_{\nu}$ is defined only for $0 < z < d$, where it is continuous, and the second and third terms on the right-hand side of Eq. (13) represent surface polarization charges that exist if the z component of \mathbf{w}_{ν} is discontinuous.

Thus the potential \bar{V}_{ν} can be found by solving Eq. (13). We write $\bar{V}_{\nu}(\mathbf{r}) = V_{\nu}(z) \exp(i\mathbf{q} \cdot \boldsymbol{\rho})$, and $V_{\nu} \equiv V_{nq}$. In a bulk semiconductor the solution is $V_{\nu} = -\chi_{\nu}/\beta$. In the heterostructure, the potential $V_{\nu} = -\chi_{\nu}/\beta$ within the slab, $V_{\nu} = 0$ beyond, is a solution for $q \neq 0$ only if $\chi_{\nu}(0) = \chi_{\nu}(d) = 0$, and hence only for the slab and reformulated slab vibrations. For the guided and interface vibrations, $V_{\nu}(z)$ extends beyond the slab. [Thus $V_{\nu}(z)$ depends on $\epsilon(z; \infty)$ beyond the slab. Consequences of this dependence are discussed in Sec. VII C and Appendix E. However, this dependence is not essential to other parts of this work, and henceforth we assume that $\epsilon(z; \infty) \equiv \epsilon(\infty)$]. For the interface vibrations, the solutions of Eq. (13) for $0 \leq z \leq d$ are given in column six of

Table I. For the guided vibrations V_{nq} is given for $0 \leq z \leq d$ by

$$-\beta V_{nq}(z) = \cos(n\pi z/d) - \exp(-qd/2) \cosh q(z-d/2) \quad (n \text{ even}), \quad (14a)$$

$$-\beta V_{nq}(z) = \cos(n\pi z/d) + \exp(-qd/2) \sinh q(z-d/2) \quad (n \text{ odd}). \quad (14b)$$

For both the guided and interface vibrations, $V_{nq}(z)$ is given beyond the slab by

$$V_{nq}(z) = V_{nq}(0) \exp(qz) \quad (z < 0), \quad (15a)$$

$$V_{nq}(z) = V_{nq}(d) \exp[q(d-z)] \quad (z > d). \quad (15b)$$

IV. SCATTERING RATES

The electron-phonon interactions calculated in Sec. III will now be applied to the evaluation of electron-phonon-scattering rates. The scattering rate of an electron from state $|i\rangle$ to state $|f\rangle$ by independent phonons in thermal equilibrium is, using Eq. (11) and Fermi's "golden rule,"

$$W = e^2 \sum_{\nu} |\langle f | \bar{V}_{\nu} | i \rangle|^2 g(\omega_{\nu}), \quad (16)$$

where

$$g(\omega) = \frac{2\pi}{\hbar} \{ N(\omega) \delta(E_f - E_i - \hbar\omega) + [1 + N(\omega)] \delta(E_f - E_i + \hbar\omega) \}, \quad (17)$$

and $N(\omega) = [\exp(\hbar\omega/kT) - 1]^{-1}$ is the phonon population factor. The scattering of an electron between states

$$|c\rangle = \psi_0(z; c) \psi_1(\rho; c) \quad (c = i, f)$$

by phonons of branch n can be expressed as a form factor^{7,20} $f_n(\mathbf{q})$, as follows:

$$e^2 \sum_{\mathbf{q}} |\langle f | \bar{V}_{nq} | i \rangle|^2 = \pi^{-1} \alpha r_p (\hbar\omega_L)^2 \frac{\omega_{nq}^2}{\omega_L^2} \times \int d^2\mathbf{q} \frac{1}{2q} n_1(\mathbf{q}) n_1^*(\mathbf{q}) f_n(\mathbf{q}), \quad (18)$$

$$f_n(\mathbf{q}) = \left| \int dz n_0(z) \beta V_{nq}(z) \right|^2 \frac{q}{I_{nq} d} \frac{\omega_L^2}{\omega_{nq}^2}, \quad (19)$$

where

$$n_1(\mathbf{q}) = \int d^2\rho \exp(-i\mathbf{q}\cdot\rho) n_1(\rho),$$

$$n_1(\rho) = \psi_1^*(\rho; f) \psi_1(\rho; i),$$

and

$$n_0(z) = \psi_0^*(z; f) \psi_0(z; i).$$

The form factor $f_n(\mathbf{q})$ expresses concisely the scattering of electrons from subband $\psi_0(z; i)$ to subband $\psi_0(z; f)$ by phonons from the branch labeled n as a function of the

in-plane momentum transfer \mathbf{q} . The total scattering by a number of branches with the same frequency is expressed by the sum over n of the corresponding $f_n(\mathbf{q})$. In the rest of Sec. IV and in Sec. V we consider the vibrations of each set to be degenerate normal modes with $\omega_{nq} = \omega_L$. Thus the factor ω_{nq}^2/ω_L^2 , which is included in Eqs. (18) and (19) for consistency with earlier definitions,^{7,20} is unity.

This method can be applied to any problem involving the polar scattering of carriers by optic phonons of a heterostructure. As an example, we consider the scattering, by the optic vibrations of a quantum well (QW), of electrons that are perfectly confined to the QW (i.e., confined by infinite potential barriers). Figure 1 shows the form factors for intrasubband scattering of electrons in the lowest subband. These form factors were calculated from Eq. (19) using the potentials given in column six of Table I. Figures 1(a)–1(c) refer to the slab, reformulated slab, and guided basis sets, respectively. The most important feature of Figs. 1(a) and 1(b) is that the curves labeled ∞

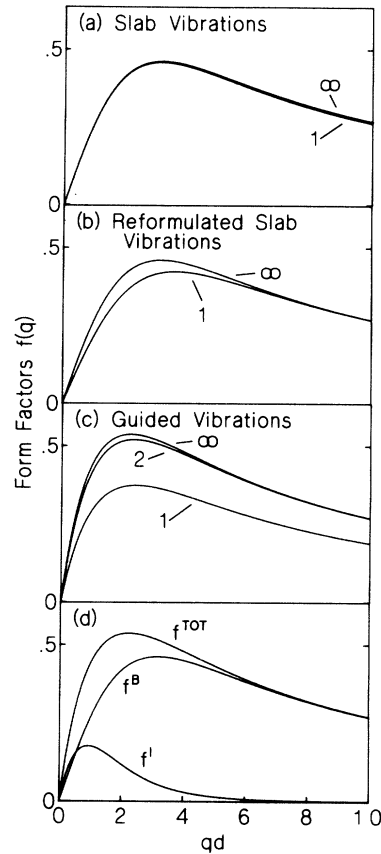


FIG. 1. Intrasubband scattering form factors for polar-optic vibrations of a quantum well plotted against qd , the product of in-plane wave vector and well width. (a), (b), and (c) refer to the different sets of vibrations given in Table I. The numerical labels give the number of symmetric vibrations that are summed to give each form factor. Thus the form factor labeled m is the sum of the individual form factors [Eq. (19)] from $n=0$ to $2m-2$. (d) shows $f^B(q)$, the total scattering form factor for bulklike vibrations; $f^I(q)$, the scattering form factor for interface vibrations; and $f^{\text{TOT}}(q) = f^B(q) + f^I(q)$.

in these two figures are identical. This is because the sum of the scattering form factors for all bulklike vibrations is the *same*, independent of the choice of basis set, as long as that set is orthogonal and complete. In other words, the total rate of scattering by all the bulklike vibrations is independent of the basis set used to describe these vibrations. This form factor summed over all bulklike vibrations is plotted separately in Fig. 1(d), in which the curves for slab and reformulated slab vibrations are superimposed and labeled f^B . Figure 1(d) also shows the scattering form factor $f^I(\mathbf{q})$ due to interface vibrations of the QW, and $f^{\text{TOT}}(\mathbf{q}) = f^B(\mathbf{q}) + f^I(\mathbf{q})$. The sum of the scattering form factors for all the guided vibrations [the curve labeled ∞ in Fig. 1(c)] is equal to $f^{\text{TOT}}(\mathbf{q})$, the sum of the interface and bulklike scattering calculated with the other basis sets. This is because the guided vibrations form a complete set, at the LO phonon frequency, that comprises both the bulklike and interface vibrations. Figure 2 shows the form factors for scattering of electrons between the first and second subbands of the QW. It can be seen that the same conclusions concerning the summed form factors apply as for the case of intrasubband scattering.

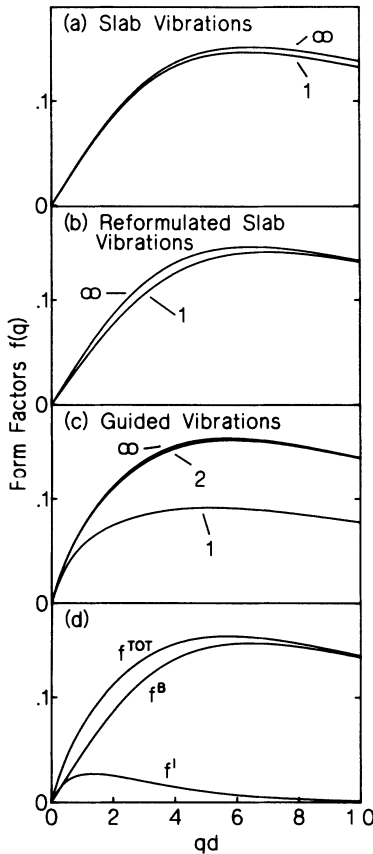


FIG. 2. Intersubband scattering form factors for polar-optic vibrations of a quantum well. The numerical labels give the number of antisymmetric vibrations that are summed to give each form factor. Thus the form factor labeled m is the sum of the individual form factors [Eq. (19)] from $n = 1$ to $2m - 1$. Other notation as Fig. 1.

V. DISCUSSION

The result that the scattering rate \mathcal{W} is independent of the basis set is unsurprising, since \mathcal{W} [Eq. (16)] is invariant under unitary transformations that mix phonon modes of the same frequency. The basis sets given in column five of Table I are orthogonal and complete, and consequently are related by unitary transformations (Appendix C).

However, much previous work¹²⁻¹⁶ is in conflict with this view. Mistakes arise either because the vibrational modes are not chosen to be an orthogonal complete set, or because the potential $\bar{V}_v(\mathbf{r})$ is calculated with incorrect boundary conditions. Rudin and Reinecke¹² have compared scattering rates calculated using different sets of vibrations, including the set suggested by Huang and Zhu,¹¹

$$\chi_{nq}(z') = \cos[(n+2)\pi z'/d] - (-1)^{n/2}, \quad n=0,2,4,\dots, \quad (20a)$$

$$\chi_{nq}(z') = \sin(\mu_n \pi z'/d) + C_n z'/d, \quad n=1,3,5,\dots, \quad (20b)$$

with $n+1 < \mu_n \leq n+2$. These vibrations are chosen, like those of Eq. (9), so that χ_{nq} and χ'_{nq} vanish at $z' = \pm d/2$. Thus they represent pure bulklike vibrations. However, the vibrations of Eq. (20) deviate from orthogonality and completeness as q is increased from zero, and this causes the scattering rates calculated using Eq. (20) to differ from those found for the slab or reformulated slab vibrations, which, according to the present work, give valid results.

Three separate errors have been made in the use of the guided vibrations. First, these vibrations form a complete set, and the scattering rate summed over guided vibrations naturally includes the scattering due to both bulklike vibrations and interface vibrations, since any bulklike vibration or interface vibration is equivalent to a linear combination of guided vibrations. It is incorrect to add to the scattering rate a separate calculation of the interface-mode scattering. Secondly, the $n=0$ vibration is usually overlooked. Thirdly, the scattering potential $V_v(z)$ is generally taken as equal to $-\beta^{-1}\chi_v(z)$. $\bar{V}_v(\mathbf{r})$ obeys Poisson's equation (13). The solution $V_v(z) = -\beta^{-1}\chi_v(z)$ has $V'_v(0) = V'_v(d) = 0$, but $V_v(0)$ and $V_v(d)$ do not vanish; thus the solution beyond the QW is

$$V_v(z) = V_v(0) \cosh qz, \quad z < 0, \\ V_v(z) = V_v(d) \cosh q(z-d), \quad z > d,$$

and does not obey the necessary boundary conditions that $V_v(\pm\infty)V'_v(\pm\infty) = 0$ except in the case $q = 0$. The solution for $V_v(z)$ that obeys these boundary conditions is the one given in Eqs. (14) and (15).

A continuum theory of optic modes in heterostructures has been proposed by Babiker and co-workers.¹⁴⁻¹⁶ This theory includes quadratic dispersion in the bulk semiconductors and uses matching conditions at each interface to treat the coupling of vibrations in adjacent layers.¹⁴ In the limit where the dispersion tends to zero with constant

ratio in the well and barrier, the normal modes in this theory are the guided vibrations of Table I, including the vibration with $n=0$, and these modes have frequency ω_L and potential $V_v = -\chi_v/\beta$. The normal modes of this dispersive theory have been used to calculate scattering rates in QW's (Ref. 15) and in superlattices.¹⁶ The modes thus found are orthogonal, and, if every mode is counted, complete. However, the theory for a GaAs/ $\text{Al}_x\text{Ga}_{1-x}$ As QW (Refs. 14 and 15) omits the GaAs-like vibrations that are not confined to the QW, i.e., those that propagate in both the $\text{Al}_x\text{Ga}_{1-x}$ As and the GaAs, apparently because Eqs. (3.7) and (3.9) of Ref. 14 do not include waves in the barriers propagating both towards and away from the QW. Thus the theory does not include all the modes that contribute to scattering. In addition, the electrostatic potential V_v in the theory of Refs. 14–16 does not obey Poisson's equation, having discontinuities at the interfaces between different materials. In the theory of Refs. 14–16, V_v is given in each material by $V_v = -\chi_v/\beta$ (using the notation of the present paper). This function obeys Poisson's equation in each individual material, but not at the interfaces. The error is part of an oversimplified treatment of the lattice mechanics (Sec. VI). For these reasons, the conclusions of Refs. 14–16 should be treated with caution, particularly where they predict a very strong dependence of scattering rates on the properties of a single member of the complete set of phonon modes (for example, the strong resonances shown in Fig. 4 of Ref. 15).

VI. CONTINUUM MECHANICS

A. Continuum mechanics of a polar slab subject to boundary conditions

The Lagrangian density for a polar material in the continuum model, with the approximations discussed in Sec. II, is

$$\begin{aligned} \mathcal{L} = & \frac{1}{2} \frac{\partial \mathbf{w}}{\partial t} \cdot \frac{\partial \mathbf{w}}{\partial t} - \frac{1}{2} \omega_T^2 \mathbf{w} \cdot \mathbf{w} + \frac{1}{2} \epsilon_0 \epsilon(z; \infty) \nabla \Phi \cdot \nabla \Phi - \gamma \mathbf{w} \cdot \nabla \Phi \\ & + \frac{1}{2} \sum_{ijkl} Z_{ijkl} \frac{\partial w_k}{\partial r_j} \frac{\partial w_l}{\partial r_i}, \end{aligned} \quad (21)$$

where $\gamma = [\epsilon_0 \epsilon(\infty) (\omega_L^2 - \omega_T^2)]^{1/2}$ and ω_T is the transverse-optic (TO) phonon frequency. The first four terms on the right-hand side of (21), from left to right, arise from the kinetic energy, the potential energy of the lattice due to short-range forces, the potential energy of the macroscopic electric field when there is no ionic motion, and the potential energy due to interaction of the lattice with the macroscopic electric field, respectively. These terms are calculated in the absence of dispersion. The final term on the right-hand side of (21) represents lowest-order (quadratic) dispersion arising from the short-range forces between ions. If this dispersion is isotropic, then

$$Z_{ijkl} = A \delta_{ij} \delta_{kl} + B \delta_{ik} \delta_{jl} + C \delta_{il} \delta_{jk}.$$

When deriving from Eq. (21) the Euler-Lagrange equations for the motion of the slab subject to BC's on \mathbf{w} at

$z=0$ and d , it is noted that the terms in \mathcal{L} that involve \mathbf{w} are defined for the slab $0 < z < d$ only. The Lagrangian is the integral of these terms over the slab, plus the integral of the $\nabla \Phi \cdot \nabla \Phi$ term over all space. Thus the Euler-Lagrange equation obtained from the variation of \mathbf{w} is

$$\frac{\partial^2 \mathbf{w}}{\partial t^2} + \omega_T^2 \mathbf{w} + \gamma \nabla \Phi + A \nabla^2 \mathbf{w} + (B + C) \nabla (\nabla \cdot \mathbf{w}) = 0 \quad (22)$$

for $0 < z < d$. The Euler-Lagrange equation obtained from the variation of Φ includes terms arising at the surface of the slab, and is

$$\nabla \cdot [\epsilon_0 \epsilon(z; \infty) \nabla \Phi - \gamma f(z) \mathbf{w}] = 0 \quad (23)$$

for all z , where $f(z) = \Theta(z) - \Theta(d - z)$, and Θ is the Heaviside step function. This is Poisson's equation, and is identical to Eq. (13) if $\mathbf{w}(\mathbf{r})$ is normalized and equal to $-\nabla \bar{\chi}$.

The solutions of the Euler-Lagrange equations that have the form $\mathbf{w} = -\nabla \bar{\chi}$ obey

$$(\omega_L^2 - \omega^2) \nabla^2 \bar{\chi} + \mu \nabla^2 \nabla^2 \bar{\chi} = 0, \quad (24)$$

$$\Phi = \frac{1}{\gamma} [(\omega_T^2 - \omega^2) \bar{\chi} + \mu \nabla^2 \bar{\chi} - B_0] \quad (25)$$

for $0 < z < d$, where $\mu = A + B + C$, and B_0 is a constant. For z beyond the slab, Φ must obey Eq. (23), which can be used to extrapolate the solution to $z = \pm \infty$.

The solutions for $\bar{\chi}$ and Φ have the form $\bar{\chi}(\mathbf{r}) = \chi(z) \exp(i\mathbf{q} \cdot \boldsymbol{\rho})$, $\Phi(\mathbf{r}) = \varphi(z) \exp(i\mathbf{q} \cdot \boldsymbol{\rho})$. Thus $B_0 = 0$ for $q \neq 0$, and for $0 < z < d$ Eqs. (24) and (25) become

$$\mu \left[\frac{d^2}{dz^2} + (\omega_L^2 - \omega^2) / \mu - q^2 \right] \left[\frac{d^2}{dz^2} - q^2 \right] \chi = 0, \quad (26)$$

$$\varphi = \frac{1}{\gamma} \left[(\omega_T^2 - \omega^2 - \mu q^2) \chi + \mu \frac{d^2 \chi}{dz^2} \right], \quad (27)$$

respectively. Equation (26) is equivalent to Eq. (10), with $(\omega_L^2 - \omega^2) / \mu - q^2$ in the role of the eigenvalue k_{nq}^2 . This equality is simply the dispersion relation

$$\omega^2 = \omega_L^2 - \mu(q^2 + k_{nq}^2), \quad (28)$$

and k_{nq} is equivalent to k , the z component of the wave vector $\mathbf{K} \equiv (\mathbf{q}, k)$. The general solution of Eq. (26) for $\chi(z)$, without regard to boundary conditions, is a linear combination of the functions $\exp(ikz)$, $\exp(-ikz)$, $\exp(qz)$, and $\exp(-qz)$. The first two functions correspond to the LO waves of the bulk solid, and k is determined from Eq. (28) for given \mathbf{q} and ω . The last two functions correspond to the interface vibrations defined in Sec. II. For given \mathbf{q} , the functional form of these latter solutions is independent of ω .

To obtain the normal modes of the slab and compare them with the solutions of Eq. (10), we consider the BC's that they must obey. The boundary conditions on \mathbf{w} and Φ that are required if the Euler-Lagrange equations are to follow from Hamilton's principle are the standard boundary conditions (SBC's) (Appendix A) for which the operators in Eqs. (22) and (23) are Hermitian. The solu-

tions of the Euler-Lagrange equations that satisfy these BC's are the normal modes of the system. \mathcal{L} is independent of x , y , and t , and we satisfy the SBC's in these domains by applying periodic BC's and then taking the infinite limit, so that the solutions are proportional to $\exp(i\mathbf{q}\cdot\boldsymbol{\rho} - i\omega t)$ with any \mathbf{q}, ω . The remaining SBC's are

$$\Phi\Phi' = 0 \quad (29)$$

at $z = \pm\infty$, and either

$$w_x = w_y = w_z' = 0 \quad (30)$$

or

$$w_x w_x' = w_y w_y' = w_z = 0 \quad (31)$$

at $z = 0$ and d . The conditions (29) on Φ are identical to the physical boundary conditions imposed in Secs. III and V. The conditions (30) and (31) on \mathbf{w} reduce if $\mathbf{w} = -\nabla\bar{\chi}$ to

$$\chi = \chi'' = 0 \quad (32)$$

and

$$\chi' = 0, \quad (33)$$

respectively. The normal modes that satisfy (29) and (32) are the slab vibrations. The normal modes that satisfy (29) and (33) do not correspond to any of the sets of vibrations given in Table I except in special cases that will be discussed below.

Analysis of the type given in Appendix B shows that, when the normal modes are not restricted to those of the form $\mathbf{w} = -\nabla\bar{\chi}$, they form a complete set for all vibrations $\mathbf{w}(\mathbf{r})$. To verify this result, it is necessary to consider the TO phonons (Appendix D 2) as well as the polar-optic (LO) phonons. The interface vibrations can be classified as either TO or LO (see Appendix D 2). When BC's (29) and (30) are satisfied, the solutions with $\mathbf{w} = -\nabla\bar{\chi}$ comprise the bulklike LO vibrations only, but the TO solutions comprise both the bulklike TO vibrations and the interface vibrations. When BC's (29) and (31) are satisfied, the solutions with $\mathbf{w} = -\nabla\bar{\chi}$ comprise both the bulklike LO vibrations and the interface vibrations, and the TO solutions comprise bulklike TO vibrations only. The bulklike LO vibrations, bulklike TO vibrations, and interface vibrations together form a complete set for all vibrations $\mathbf{w}(\mathbf{r})$.

The solutions of Eq. (10) discussed in Sec. II are not the same as the solutions of the Euler-Lagrange equations, even though it is shown above that the Euler-Lagrange equations reduce to Eq. (10) when Φ is eliminated. The solutions are different because the SBC's for Eq. (10) are not the same as those for the Euler-Lagrange equations. The SBC's for Eq. (10) (Sec. II and Appendix A) are sufficient to satisfy the \mathbf{w} -related SBC's for Eqs. (22) and (23). The solutions of Eq. (10), subject to the SBC's for this equation, are thus normal modes if and only if the unique electric potential derived from Eq. (27) and extrapolated beyond the slab using Eq. (23) obeys $\varphi(\pm\infty)\varphi'(\pm\infty) = 0$ [when this is true, the solutions of Eqs. (27) and (13) coincide]. This condition is satisfied by the slab vibrations but not in general by the reformulated

slab vibrations or the guided vibrations.

In other words, the SBC's for Eq. (10) together with the BC (29) overdetermine the normal modes in some circumstances. When this is true, the solutions of Eq. (10) are not normal modes. The conditions (33) at $z = 0$ and d and (29) at $z = \pm\infty$ are sufficient to satisfy the SBC's for Eqs. (22) and (23) and hence to produce normal modes: additional BC's are not required. There is only one set of normal modes that satisfies these conditions. In general, these modes obey neither $\chi(0) = \chi(d) = 0$ nor $\chi'''(0) = \chi'''(d) = 0$ and so are neither the reformulated slab vibrations nor the guided vibrations.

The boundary conditions that $\chi_v' = \chi_v''' = 0$ at $z = 0$ and d , and $\varphi_v \varphi_v' = 0$ at $z = \pm\infty$, are incompatible except in the case $q = 0$, and consequently the guided vibrations with $q \neq 0$ are not the normal modes of the slab in any circumstances. The guided vibrations with $\varphi_v = -\beta^{-1}\chi_v$ are solutions of the Euler-Lagrange equations, but, as noted in Sec. V, this φ_v does not obey the correct BC's at $z = \pm\infty$ except in the case $q = 0$.

The modes that obey Eqs. (33) and (29) do correspond to solutions of Eq. (10) in special cases. As $q \rightarrow 0$ the modes with $\omega \approx \omega_L$ tend towards the guided vibrations with $n \neq 0$, and as $\mu \rightarrow 0$ (infinitesimal dispersion) the $q \neq 0$ modes tend towards the reformulated slab vibrations.

B. Continuum mechanics of a polar heterostructure

The continuum theory given in Sec. VIA is a useful model of the motion of an ionic layer subject to BC's at its interfaces, as long as the approximations of quadratic and isotropic dispersion are acceptable. Quadratic dispersion is valid for a semiconductor slab if the wave vector (\mathbf{q}, k) is not too large, or alternatively if the dispersion is taken to be infinitesimal. The relation of the slab, reformulated slab, and guided vibrations to the normal modes of the layer subject to BC's is found, without recourse to microscopic theories. However, this method does not tell us which BC's follow from the mechanics of the heterostructure as a whole, and so it does not give a theoretical justification for the reformulation of the slab vibrations. For this purpose it is necessary to consider the mechanics of the entire structure, and deduce the connection rules that relate the fields on either side of an interface.

Several authors have investigated the connection rules by comparison of macroscopic and microscopic theories. Huang and Zhu¹¹ examined the solutions of a microscopic model of the lattice mechanics and found that, in the zero-dispersion limit with \mathbf{q} neither too large nor zero, the normal modes are closely approximated by the interface modes and the reformulated slab vibrations. A similar approach was adopted in Ref. 21. Tsuchiya, Akera, and Ando²² have developed a slightly different method, which uses a dynamical equation equivalent to Eq. (22) (but including anisotropy) and imposes either the BC $\mathbf{w} = 0$ at the faces of the slab or connection rules derived from microscopic theory. In the first case, the results were compared with those of microscopic calculations, with good agreement. In a continuum theory of the

zero-wave-vector modes of a superlattice, Gerecke and Bechstedt²³ obtain both the equation of motion and the connection rules by comparison with a simple microscopic theory.

The connection rules that relate the fields on either side of an interface can also be derived from a continuum theory. For the continuum mechanics of the heterostructure as a whole, \mathbf{w} is defined everywhere (in contrast to the treatment of Sec. VIA, in which \mathbf{w} is defined for $0 < z < d$ only, with BC's imposed at $z=0$ and d). The simplest case is when the forces are the same throughout the structure, and only the atomic masses vary from one layer to the next. The forces are then the same as for a bulk material, with no interface-related terms. This approximation is sometimes used in microscopic theories of superlattice vibrations²⁴ with good results. The dispersive term in the Lagrangian density is then

$$\frac{1}{2} \sum_{ijkl} \rho Z_{ijkl} \frac{\partial}{\partial r_j} (\rho^{-1/2} w_k) \frac{\partial}{\partial r_i} (\rho^{-1/2} w_l),$$

where ρZ_{ijkl} is independent of z , so that ρA , ρB , and ρC are constants. The Euler-Lagrange equations reduce to (22) and (23) within each layer. At an interface the equations are equivalent to connection rules, which relate the fields on either side of the interface. If $A \neq 0$, $A + B + C \neq 0$ (i.e., both the LO and TO bulk modes have nonzero dispersion), then the connection rules are that $\rho^{-1/2} \mathbf{w}$, $(\rho^{-1/2} \mathbf{w})'$, Φ , and $D_z = \epsilon_0 \epsilon(z, \infty) \Phi' - \gamma w_z$ are continuous, where \mathbf{D} is the electric displacement.

Use of these connection rules ensures that the set of normal modes is orthogonal and complete, because the rules follow from the Euler-Lagrange equations. Sections IV and V show that the orthogonality and completeness properties of the normal modes are essential if electron-phonon scattering rates are to be calculated accurately; but "modes" do not necessarily have these properties unless the connection rules are derived from valid Euler-Lagrange equations.

The connection rules have been obtained by applying Lagrangian mechanics^{25,26} and the usual method of solving differential equations with discontinuous terms (Ref. 27, Chap. 11.10). The rules for $\rho^{-1/2} \mathbf{w}$ and $(\rho^{-1/2} \mathbf{w})'$ are equivalent to the familiar condition that the net force on the interface is zero.²⁶

There has been some debate over whether the connection rules that govern optic modes in a heterostructure are mechanical BC's or electromagnetic BC's.^{9,13,17,18} In a nondispersive theory¹⁰ \mathcal{L} has no terms involving spatial derivatives of \mathbf{w} , and so there are no mechanical BC's in this case. The only BC's are the electromagnetic BC's that Φ and D_z are continuous. The present discussion of the dispersive continuum theory has shown that, with no contradiction, mechanical BC's apply to \mathbf{w} and its derivatives, while electromagnetic BC's apply to Φ and \mathbf{D} . These conditions do not conflict if all the solutions of the dispersive continuum theory are retained. However, in Refs. 14–16 the mechanical BC's and electromagnetic BC's are contradictory, and the latter are violated. The treatment of Refs. 14–16 initially includes retardation, and the solutions are labeled either "longitudinal" [solutions of Eq. (2.14) of Ref. 14] or "transverse" [solutions of

Eq. (2.13) of Ref. 14]. The "transverse" solutions are discarded; but these solutions include the polaritons that tend to the interface vibrations of the present work when retardation is neglected (Appendix D 3). The remaining "longitudinal" waves correspond to the LO waves of the bulk solid, and have the form

$$\mathbf{w} = w_0 \hat{\mathbf{K}} \exp(i \mathbf{K} \cdot \mathbf{r} - i \omega t),$$

$$\nabla \Phi = \left[\frac{\omega_L^2 - \omega_T^2}{\epsilon_0 \epsilon(\infty)} \right]^{1/2} \mathbf{w},$$

where the theory of Refs. 14–16 requires that $\omega(k)$ is given by a dispersion relation of the form $\omega^2 = \omega_L^2 - \mu k^2$, and that $\nabla \cdot \mathbf{w} \neq 0$ so that $k^2 \neq 0$. The approach used in Refs. 14–16 is to construct normal modes solely from these "longitudinal" solutions (which, incidentally, are independent of retardation). But these "longitudinal" waves do not provide sufficient degrees of freedom to satisfy mechanical and electromagnetic BC's simultaneously. A normal mode of a heterostructure can be written within a single layer as a linear combination of all the bulk waves with the correct frequency and \mathbf{q} : in the present (nonretarded) theory, LO, TO, and interface vibrations; in the retarded theory of Refs. 14–16, "longitudinal" and "transverse" vibrations. The neglect of the "transverse" (polariton) vibrations in Refs. 14–16 would lead to contradictions in the treatment of a heterostructure (i.e., more equations than unknowns in the matching problem at an interface), except that the boundary conditions are chosen, arbitrarily, to be those for hydrodynamic fluid flow rather than those for a solid-state semiconductor heterostructure. Electromagnetic BC's are completely ignored. These are the main errors made in Refs. 14–16.

The Lagrangian density \mathcal{L} of the present work differs from that given in Ref. 14. The fundamental equations of Ref. 14 within a single material are the equations of motion, i.e., the dispersive Born-Huang equations together with Gauss's law, rather than an expression for \mathcal{L} . These equations are in fact equivalent to the Euler-Lagrange equations of the present work, Eqs. (22) and (23). However, as discussed above, Refs. 14–16 discard some of the solutions of these equations when constructing LO modes. \mathcal{L} is chosen in Ref. 14 to be consistent only with the "longitudinal" solutions of that work, and is a simplified expression that is not valid for all the vibrations of the slab.

Continuum theories of the mechanics of a heterostructure are problematic because waves with small k often couple to waves for which $\text{Re}k$ lies beyond the bulk Brillouin-zone boundary. Since the latter are unphysical, this cannot be a satisfactory description of the mechanics. The GaAs-like normal modes of a GaAs/AlAs heterostructure, for example, will include such vibrations of the AlAs if the quadratic dispersion is set to its experimental value.²⁸ One might attempt to solve this problem by modeling the bulk dispersion with an expression that is more accurate than a quadratic. To do this, dispersive terms that are higher order in $\partial/\partial r_i$, and hence in the wave vector (\mathbf{q}, k) , must be included in the Lagrangian density. Anisotropic terms can also be included.²² The

problem with higher-order terms is that n th-order dispersion will give $3n + 2$ connection rules, and when matching at an interface the extra conditions can only be satisfied by including the bulk solutions for which $\text{Re}k$ lies beyond the Brillouin-zone boundary of the bulk semiconductor [for specific \mathbf{q}, ω , n th-order dispersion gives $3n + 2$ optic-phonon vibrations in the (complex- k) phonon band structure]. These are valid solutions of a continuum problem, but do not correspond to vibrations of a lattice with finite unit cell. The problem of waves with $\text{Re}k$ beyond the bulk Brillouin-zone boundary is thus common to both quadratic and higher-order dispersive continuum theories. It is a fundamental problem of continuum models if the solutions are required to satisfy the principles of continuum mechanics (which at least ensure the orthogonality and completeness of modes) rather than merely to resemble the solutions of microscopic theories. It appears that, except in special cases (e.g., infinitesimal dispersion), the mechanics of a heterostructure, including the connection rules, is essentially microscopic. However, the theory of quadratic dispersion will be examined further, since the case of infinitesimal dispersion does give a useful insight into the properties of normal modes in real heterostructures.

C. Connection rules in the limit of infinitesimal dispersion

The bulklike vibrations are degenerate normal modes in the nondispersive theory. The way in which this degeneracy is lifted by dispersion can be found from the connection rules in the limit of infinitesimal dispersion. We consider these rules at a junction between materials 1 and 2. The bulk LO(Γ) and TO(Γ) frequencies in material i ($i = 1, 2$) are ω_{L_i} and ω_{T_i} , respectively. In material i , each normal mode (for given in-plane wave vector \mathbf{q} , frequency ω) is a linear combination of eight different vibrations: two LO and four TO vibrations corresponding to phonons from the complex band structure of the bulk material i ; and the two interface vibrations. It is convenient to class the TO vibrations as either transverse electric²⁹ (TE) or transverse magnetic²⁹ (TM); the four TO vibrations comprise two TE and two TM waves. When we take the zero-dispersion limit of the mechanics, we must distinguish between “slowly varying” and “rapidly varying” components of the normal mode. The rapidly varying components are the vibrations that belong to the bulk optic-phonon branches \mathcal{B} whose frequencies, in the absence of dispersion, are separated from ω by a finite amount. These rapidly varying components are either oscillatory or evanescent, depending on the sign of the dispersion, with a value of k (the z component of the wave vector) that tends to infinity in the zero-dispersion limit. The slowly varying components are the two interface vibrations plus any of the six optic vibrations that have finite wave vector in the zero-dispersion limit. We shall now discuss how, in the limit of infinitesimal dispersion, the rapidly varying components can be eliminated from the calculation, giving simplified connection rules that relate the slowly varying fields on either side of the interface.

The sign of the dispersion of the branches \mathcal{B} is chosen

so that at \mathbf{q}, ω the rapidly varying components are all evanescent, i.e., all have imaginary k . This restriction is necessary within a continuum theory so that the modes do not have the unphysical components (oscillatory with k beyond the Brillouin zone) mentioned in Sec. VI B. Each branch belonging to \mathcal{B} contributes two evanescent vibrations, one growing and the other decaying away from the interface over a length scale whose zero-dispersion limit is zero. In the limit of infinitesimal dispersion, the components of the normal modes due to the *growing* vibrations are not significant at the interface and are discarded. In the same limit, the *decaying* vibrations correspond to discontinuities in some of the fields and their derivatives, so that some of the finite-dispersion connection rules do not apply to the slowly varying fields in the limit of infinitesimal dispersion.

The connection rules for the slowly varying fields in the limit of infinitesimal dispersion depend on which of the vibrations in each layer are rapidly varying. For $\omega \approx \omega_{L_2}$ (i.e., so that the zero-dispersion limit of k_{nq} [Eq. (28)] is finite), the numbers of such vibrations that are *decaying* away from the interface are two in layer 2 (the TE and TM vibrations) and three in layer 1 (the TE, TM, and LO vibrations). The same numbers of exponentially *growing* waves are discarded. The discontinuous quantities can be found from Table II. For $\omega \approx \omega_{L_1}$, the rapidly decaying vibrations produce arbitrary discontinuities in $(\rho^{-1/2}\mathbf{w})'$, $\rho^{-1/2}w_x$, and $\rho^{-1/2}w_y$, so that the connection rules that relate the slowly varying components of the fields on either side of the interface reduce to the continuity of Φ , D_z , and $\rho^{-1/2}w_z$.

The connection rules can similarly be derived at other

TABLE II. Discontinuities in the conserved quantities $\mathbf{u} = \rho^{-1/2}\mathbf{w}$ and \mathbf{u}' due to rapidly decaying evanescent vibrations. The quantities that are discontinuous can be found from this table by counting, at the frequency of interest, the rapidly decaying evanescent waves of each polarization. The table entries are derived from the zero-dispersion limit of the different evanescent waves. A single rapidly decaying evanescent wave of a particular polarization (on either side of the interface) produces a discontinuity in one component of \mathbf{u}' . A second rapidly decaying wave of the same polarization (on the other side of the interface) allows in addition discontinuities in the same component of \mathbf{u} and (except for TE waves) in a different component of \mathbf{u}' , the sizes of these additional discontinuities being related. Now, if ω_{T_1} , ω_{L_1} , ω_{T_2} , and ω_{L_2} are all unequal, then at any frequency there is at least one rapidly decaying wave of each polarization, and so u'_x , u'_y , and u'_z are all discontinuous. Since the size of these discontinuities is arbitrary, the discontinuities in \mathbf{u}' due to additional rapidly decaying waves are immaterial. Rapidly varying evanescent waves do not give rise to discontinuities in Φ or D_z .

Rapidly decaying wave	Discontinuous quantities
Single TE wave	u'_y
Single TM wave	u'_x
Single LO wave	u'_z
Additional TE wave	u_y
Additional TM wave	u_x, u'_z
Additional LO wave	u_z, u'_x

phonon frequencies. The rules for $\omega \approx \omega_{Ti}$ are that Φ , D_z , $\rho^{-1/2}w_x$, and $\rho^{-1/2}w_y$ are continuous. If ω is not close to any bulk optic-phonon frequencies, then only Φ and D_z are continuous.

These connection rules in the limit of infinitesimal dispersion do not contradict those of the nondispersive theory.¹⁰ Away from $\omega = \omega_{Ti}$ and ω_{Li} , the connection rules are the same in the two theories, and so in this frequency range the normal modes of the dispersive theory are the usual interface modes. The effect of the additional connection rules that arise close to a bulk optic-phonon frequency is simply to lift the degeneracy of the bulklike optic modes, and at small q to govern the mixing between interface and bulklike modes.

These connection rules for slowly varying fields will be applied to LO modes in Sec. VID, to TO modes in Appendix D 2, and to LO modes in a retarded theory in Appendix D 3.

D. Application to LO modes of a quantum well

The LO modes of a hypothetical GaAs/AlAs QW can be found by applying the connection rules derived in Sec. VIC. For the antisymmetric modes with frequency close to the GaAs LO frequency, the slowly varying field components can be written within each layer as $\mathbf{w} = -\nabla\chi$, $\chi(\mathbf{r}) = \chi(z)\exp(iqx)$, where

$$\chi = \begin{cases} F \exp(-qz'), & z' > d/2 \\ \frac{G}{k} \sin kz' + H \sinh qz', & -d/2 < z' < d/2. \end{cases} \quad (34)$$

Applying the connection rules for Φ , D_z , and u_z leads to a secular equation for k . The distinction made in Sec. VIC between slowly varying and rapidly varying fields is valid only in the limit of infinitesimal dispersion, which for modes with $\omega \approx \omega_{L2}$ means

$$|\omega_{L2}^2 - \omega_{T1}^2|/A, \quad |\omega_{L2}^2 - \omega_{T2}^2|/A, \quad |\omega_{L2}^2 - \omega_{L1}^2|/\mu \gg (k^2 + q^2). \quad (35)$$

Making this approximation, the secular equation becomes

$$\frac{1}{k} \sin \frac{kd}{2} = \frac{1}{q} \cos \frac{kd}{2} \left[\tanh \frac{qd}{2} - N\mu(k^2 + q^2) \right], \quad (36)$$

where

$$N = \frac{\epsilon_2(\infty)(\omega_{T1}^2 - \omega_{L2}^2)}{\epsilon_1(\infty)(\omega_{L2}^2 - \omega_{T2}^2)(\omega_{L1}^2 - \omega_{L2}^2)},$$

and the subscripts 1 and 2 refer to the barrier (AlAs) and the well (GaAs), respectively. We take $\epsilon_1(\infty) = 8.16$,³⁰ $\nu_{L1} = 404 \text{ cm}^{-1}$, $\nu_{T1} = 361 \text{ cm}^{-1}$,³¹ $\epsilon_2(\infty) = 10.89$,³² $\nu_{L2} = 292 \text{ cm}^{-1}$, $\nu_{T2} = 268 \text{ cm}^{-1}$,³³ where $\nu = \omega/2\pi c$. k is related to the phonon frequency ω by Eq. (28). Calculations were performed for a 100-Å QW with the properties of GaAs/AlAs except that the dispersion μ is set to a value of $10^{-14}(2\pi c)^2$ rather than the experimental value²⁸ for $\mathbf{K} \parallel [001]$ of $2.0 \times 10^{-12}(2\pi c)^2$. The solutions of Eq.

(36) are plotted in Figs. 3 and 4. The dispersion shown in Fig. 3 is of most interest and will be discussed in some detail later.

Similar analysis for the symmetric modes shows that their dispersion relation is

$$\tan \frac{kd}{2} = -\frac{q}{k} \tanh \frac{qd}{2}, \quad (37)$$

which is the condition for symmetric reformulated slab vibrations. Hence for $qd \ll 1$ the frequency depends only weakly on q , and does not have the complex behavior found for the antisymmetric modes and shown in Fig. 3. In the limit as $qd \rightarrow 0$ (and approximately true for all $qd \ll 1$), condition (37) becomes

$$\sin \frac{kd}{2} = 0 \quad (k \neq 0), \quad (38)$$

and the symmetric reformulated slab vibrations tend to the symmetric guided vibrations with $n \neq 0$.

In analyzing the results for antisymmetric modes, it is useful to know the dispersion relation of antisymmetric GaAs-like interface modes calculated when the bulk dispersion is zero. This dispersion relation is²⁰

$$\frac{\epsilon_2(\omega)}{\epsilon_1(\omega)} = -\tanh \frac{qd}{2},$$

which becomes, on substitution of ϵ_1 and ϵ_2 and making the approximation (35)

$$\omega_{L2}^2 - \omega^2 = -\frac{1}{N} \tanh \frac{qd}{2}.$$

Using Eq. (28), this gives

$$\left[\tanh \frac{qd}{2} - N\mu(k^2 + q^2) \right] = 0. \quad (39)$$

This interface-mode condition is shown as a dotted line in Fig. 3.

These results lead to the following conclusions:

(i) At small q , the dispersion relation for antisymmetric

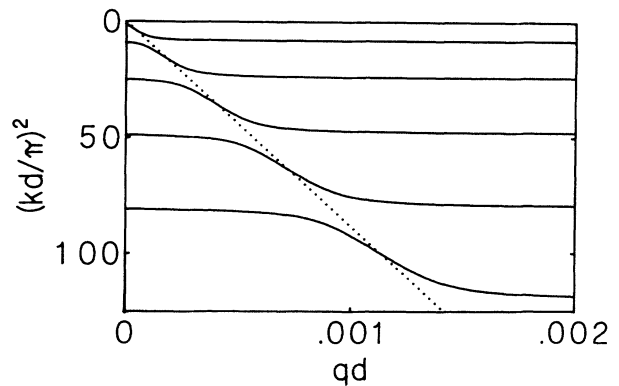


FIG. 3. Solid lines are dispersion curves of antisymmetric GaAs-like LO modes in a 100-Å GaAs/AlAs QW with weakened dispersion (see text). For ease of interpretation, $(kd/\pi)^2$ rather than the frequency is plotted on the y axis. This quantity is accurately proportional to the difference in frequency from ν_{L2} . Using Eq. (28) and the values given in the text, $(kd/\pi)^2 = 0$ corresponds to the frequency $\nu_{L2} = 292 \text{ cm}^{-1}$, $(kd/\pi)^2 = 100$ is a frequency 0.0169 cm^{-1} smaller. The dotted line is the antisymmetric GaAs-like interface mode calculated in the absence of bulk dispersion from Eq. (39).

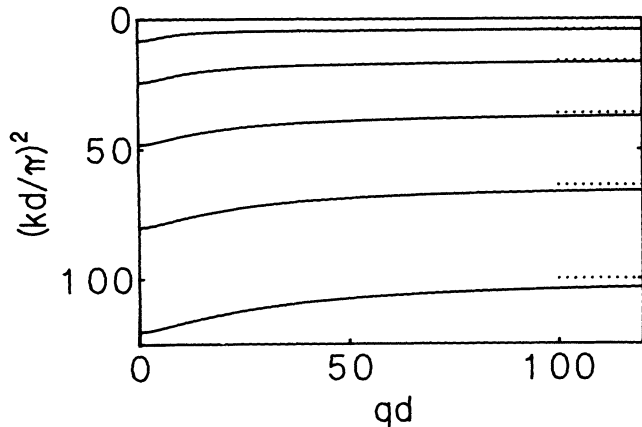


FIG. 4. Solid lines are dispersion curves of antisymmetric GaAs-like LO modes in a 100-Å GaAs/AlAs QW with weakened dispersion (see text). $(kd/\pi)^2$ is plotted on the y axis, as in Fig. 3. Note that the units of the horizontal scale are different from those of Fig. 3. qd is large, and the frequency relative to ν_{L2} has contributions from both k and q [Eq. (28)]. In the 100-Å QW the Brillouin-zone boundary is at $qd \approx 111$. The dotted lines correspond to even-integer values of kd/π , and are the large- qd limits of the dispersion curves (see text).

modes is dominated by the second term in the large parentheses in Eq. (36). As $q \rightarrow 0$, the relation tends to

$$\cos \frac{kd}{2} = 0, \quad (40)$$

and the modes tend towards the antisymmetric guided vibrations.

(ii) At “large” q [defined in (v) below], the dispersion relation for antisymmetric modes is dominated by the first term in the large parentheses in Eq. (36), and tends to

$$\frac{1}{k} \tan \frac{kd}{2} = \frac{1}{q} \tanh \frac{qd}{2}. \quad (41)$$

This is the condition for antisymmetric reformulated slab vibrations. These vibrations become the normal modes because as q increases, the continuity of Φ , D_z and u_z requires the fields outside the QW to be weak [$F \rightarrow 0$ in Eq. (34)], and so the strong fields are confined to the GaAs well. Hence the continuity conditions reduce to

$$\chi = \chi' = 0 \quad (42)$$

at $z' = \pm d/2$, which are the BC’s for the reformulated slab vibrations (Sec. II).

(iii) The dispersion exhibited in Fig. 4 follows directly from Eq. (41) and is a property of the reformulated slab vibrations. As long as the bulk dispersion is small [Eq. (35)], its strength determines the mode frequencies in the regime of Fig. 4 only through the factor μ in Eq. (28), and does not affect the qd dependence of kd for a given phonon branch.

When $q \gg k$, kd/π tends to an even integer. These limiting values are marked with dotted lines in Fig. 4. In the $q \gg k$ regime the interface vibrations are rapidly varying with respect to z , and so the only slowly varying

term left from Eq. (34) is $\chi = (G/k) \sin kz'$, and the BC’s (42) on this slowly varying term simplify to $\chi = 0$ at $z' = \pm d/2$. Thus at large q the reformulated slab vibrations tend towards the slab vibrations. Figure 4 shows that, except for the highest-frequency modes in wide QW’s, the regime in which the slab vibrations are the normal modes has not been reached even for q at the Brillouin-zone boundary. Thus the slab vibrations are not a good description of the confined modes of a heterostructure.

(iv) At still larger q , the second term in the large parentheses in Eq. (36) dominates the first, but the value of q is inconsistent with the assumption (35), and so the connection rules for the slowly varying fields have broken down and Eq. (36) is invalid. This regime is thus beyond the scope of the infinitesimal-dispersion limit, which can be restored by reducing the value of μ .

(v) Both in the small- q regime of Eq. (40) and in the $qd \ll 1$ part of the “large- q ” regime of Eq. (41), the frequency depends only weakly on q . The crossover between these two regimes occurs when the two terms in the large parentheses in Eq. (36) are of approximately equal magnitude, and corresponds to the steeply sloping part of the dispersion curves of Fig. 3. The crossover condition is identical to Eq. (39), and thus corresponds to the interface-mode dispersion curve calculated in the absence of bulk dispersion. The crossover between the small- q and “large- q ” regimes occurs for given k at $qd \ll 1$ because the bulk dispersion μ is infinitesimal. In the crossover regime, the modes have a large projection onto interface vibrations.

Equation (35) suggests that the experimental dispersion of GaAs is too large for this small-dispersion theory to be applied, except for the highest-frequency modes in wide (~ 100 -Å) QW’s. A reduced value of μ is used in Figs. 3 and 4 to ensure high accuracy for all the modes plotted. The conclusions for this case of weak dispersion give the following insights into the behavior of the modes of practical heterostructures (i.e., those with thin layers and the correct value of dispersion).

(vi) The dispersive behavior of the antisymmetric modes in the crossover regime can be considered as due to the interaction of the bulklike modes with the GaAs-like antisymmetric interface mode. This behavior is particularly clear at high values of k , for the following reason. Section IV shows that the electron-phonon scattering by guided vibrations or reformulated slab vibrations is very weak at large k (i.e., large n in Table I); thus the scattering by the large- k modes of Eq. (36) is strong only in the crossover regime in which the modes have a large projection onto interface vibrations. The interface mode no longer exists as a distinct branch in the presence of bulk dispersion because of the interface-bulklike interaction (Fig. 3). However, the existence of the interface “mode” can be inferred from this behavior of the electron-phonon scattering.

This large- k behavior indicates the nature of the interface “modes” when, unlike in the discussion of interface modes in Sec. VI C, the sign of the dispersion is such that bulklike LO and interface modes occupy the same frequency band. The interface “mode” exists in the sense

mentioned in the preceding paragraph, although the true normal modes are not simple interface modes and obey mechanical BC's in addition to the continuity of Φ and D_z .

The bulklike dispersion can never be considered a small perturbation because it lifts the degeneracy of the bulklike modes and strongly mixes the bulklike and interface modes. Raman scattering can probe both these effects.⁹ However, if the frequency resolution of an experiment is not adequate to resolve the individual phonon branches of Fig. 3, then a frequency-resolved and wave-vector-resolved measurement of the electron-phonon interaction will give very similar results with and without bulk dispersion; in particular, the coupling will be strong close to the LO and interface-mode frequencies only.

(vii) The symmetric modes with $\omega \approx \omega_{L2}$ do not exhibit interface-bulklike mixing, because there are no symmetric interface modes at this frequency. The normal modes are approximately equal to the reformulated slab vibrations (they become exactly equal as $\mu \rightarrow 0$). In the same way as for the "large- q " antisymmetric modes, this result follows from the weakness of the fields outside the QW. Equation (37) shows that at $q \sim k$ the symmetric modes have dispersion similar in nature and in origin to that found for the antisymmetric modes in this wave-vector range and shown in Fig. 4.

(viii) The $q=0$, $\omega \approx \omega_{L2}$ modes are the guided vibrations with $n \neq 0$, in agreement with the findings of Raman backscattering.⁹ The difference between the modes at $q=0$ and at $q \neq 0$ has been examined in microscopic theories⁸ but has not previously been explained by equations of motion and connection rules derived entirely from continuum mechanics.

The set of vibrations with $\mathbf{w} = -\nabla\bar{\chi}$ at $q=0$ is completed by the $n=0$ guided vibration, which is equivalent at $q=0$ to the symmetric interface vibration. In a non-dispersive theory this vibration corresponds to the interface mode at $\omega = \omega_{T2}$. In a dispersive theory it contributes to the TM modes near $\omega = \omega_{T2}$, just as the antisymmetric interface vibration contributes to the LO modes near $\omega = \omega_{L2}$.

The modes change in character from guided vibrations to reformulated slab vibrations as q increases from zero. The most rapid change occurs when the interface-mode dispersion curve is crossed. In the limit of infinitesimal dispersion, the modes at $q \neq 0$ can be taken to be the reformulated slab vibrations and the interface modes.

(ix) The way in which the strongly dispersive interface modes interact with the weakly dispersive antisymmetric bulklike modes is typical of optic modes in heterostructures. This interpretation of dispersion curves was first given for the zero-wave-vector angular dispersion of optic modes in a superlattice, which has been studied theoretically by many methods.^{8,22,23} The zero-wave-vector superlattice dispersion is the interface-bulklike-interaction effect that is probably most amenable to study by Raman scattering, since large scattering wave vectors are not required. However, a Raman study of the interface-bulklike interaction in this or any other system has the complication that some experiments must be performed in an off-axis geometry.³⁴

VII. CONCLUSIONS

A. Lattice mechanics

Section VI gives a continuum treatment of the lattice mechanics of polar heterostructures. It discusses the continuum mechanics of a polar slab subject to SBC's. However, the most useful results of Sec. VI are those for the continuum mechanics of a complete heterostructure in the case of infinitesimal dispersion. These results will now be summarized.

It has been shown that, contrary to previous suggestions,^{14-16,35} there is no contradiction between the mechanical BC's that apply to \mathbf{w} and its derivatives, and the electromagnetic BC's that apply to Φ and \mathbf{D} . Both types of BC must be applied in order to deduce the normal modes of a heterostructure.

It is found that the LO modes are governed by the connection rules that Φ , D_z , and u_z are continuous at each interface. Except for the case of antisymmetric modes with small q (less than or comparable to the q value of the zero-bulk-dispersion interface mode with the same frequency), these connection rules reduce to the conditions $\chi_v = \chi'_v = 0$ at $z=0$ and d . Thus, in the limit of infinitesimal dispersion, the polar-optic modes at $q \neq 0$ can be taken to be the reformulated slab vibrations and the interface modes. This justifies the idea¹¹ of reformulating the slab vibrations, contrary to the criticism of Refs. 35 and 36.

In the $q \rightarrow 0$ limit, the LO modes (if symmetric, the reformulated slab vibrations; if antisymmetric, the exceptional case mentioned in the previous paragraph) tend towards the guided vibrations with $n \neq 0$, ensuring that these are the $q=0$ modes that are detected in Raman-backscattering experiments.^{9,37}

These results are obtained in an entirely continuum theory, without recourse to microscopic calculations. The theory also neglects electromagnetic retardation; i.e., it gives an electrostatic treatment. The results show that a consistent treatment of the lattice mechanics and the electron-phonon scattering can be given within this framework. It is shown in Appendix D3 that electromagnetic retardation has significant effects on LO modes only at very small q , close to the light line. The effect of retardation on polar-optic scattering rates is insignificant, and its treatment is an unnecessary complication.

Very recently, Ridley³⁶ has proposed a continuum model of the optic modes that uses elastic rather than hydrodynamic¹⁴⁻¹⁶ BC's. Although this new model addresses some of the problems of Refs. 14-16, its starting point is the bulk dispersion relations for optic modes rather than equations of motion with both mechanical and electromagnetic terms, and so it leaves open the question of whether LO modes should obey electromagnetic BC's.

B. Electron-phonon scattering

The most important requirement of a set of polar-optic vibrations used as normal modes in a continuum theory of electron-phonon scattering is that it should be orthog-

onal and complete. In addition, the electrostatic potential associated with each vibration should obey Poisson's equation with the correct boundary conditions. Claims of reduced scattering rates or other novel properties should be treated with caution unless they employ a phonon basis set that fulfills these requirements. For a thermal-equilibrium independent-phonon property, such as a low-field carrier mobility or an intersubband transition rate, any such basis set for the degenerate bulklike modes in a nondispersive model of the optic phonons will give the same result. For properties that are not sensitive to differences in the phonon energy on the scale of the LO dispersion, this invariance should remain a good approximation even when dispersion is included, and so knowledge of the normal modes is not needed to calculate scattering rates.

In assessing the accuracy of scattering rates calculated with a continuum basis set, it is interesting to note that nearly all the electron-phonon scattering arises from the one or two phonon branches, of the correct parity, with smallest n (Figs. 1 and 2). Except in slabs with a very small number N of molecular monolayers, a continuum model will give a good approximation to the atomic displacements and the scattering for these "long-wavelength" (small- n) vibrations.³⁸ Thus scattering rates calculated with a continuum basis set will accurately account for polar electron-phonon interactions except in heterostructures with very thin layers (e.g., very-short-period superlattices). The basis set need not correspond to the normal modes except when high spectral resolution of the phonons (as in Raman scattering⁹) reveals how the different bulklike and interface vibrations are mixed to form each individual mode.

Any of the three complete sets of vibrations given in column five of Table I can validly be chosen as a basis set, for each layer of a heterostructure, and used to calculate the rates of electron-phonon scattering by the nearly degenerate LO modes of the layer. Calculations of electron-phonon scattering using the slab vibrations^{10,39} (together with the interface modes) as the normal modes give valid results, are simple, and are free of pitfalls, as long as the scattering is not required with frequency resolution high enough to resolve the individual bulklike LO modes. It is paradoxical that this should be so when experiments,⁹ microscopic calculations,^{8,11} and continuum mechanics (Sec. VI) show that the slab vibrations are not the normal modes of a semiconductor layer in a heterostructure. Calculations with the slab vibrations are valid because these form a complete orthogonal set for the approximately degenerate polar-optic vibrations at $\omega \approx \omega_L$.

C. Phonon band-structure engineering

These results demonstrate that, although in the design of a heterostructure of similar semiconductors it may be possible to alter the form of individual phonon modes, it is much more difficult to exploit this alteration to engineer thermal-equilibrium electron-phonon scattering rates because these rates are approximately invariant with respect to transformations among nearly degenerate modes. This means that any decrease in the scattering by one mode will be compensated by an increase in the

scattering by other modes. This phonon band-structure engineering is discussed in more detail in Ref. 20, where the modes that are *not* degenerate with the bulklike modes, i.e., the interface modes, are also discussed. Reference 20 shows that the coupling of the interface vibrations of different layers to form the interface modes (not discussed in the present work) offers little scope for the manipulation of electron-phonon-scattering rates. Indeed, when calculating electron-phonon scattering, it is a good approximation²⁰ to assume that the interface modes are pure interface vibrations of each layer, with frequency equal to the LO phonon frequency for that layer [this is called the LO phonon approximation (LPA) in Ref. 20]. Scattering rates differ from those calculated in the LPA because the phonon frequencies are not equal to the bulk LO frequencies, because a mode comprises vibrations in more than one material, and because of retardation, but these differences are expected to be small. The possible techniques for designing thermal-equilibrium electron-phonon-scattering rates in semiconductor heterostructures are shown²⁰ to be (i) the design of electron (rather than phonon) wave functions and energy levels, i.e., conventional band-structure engineering, and (ii) phonon band-structure engineering, which is limited to the obvious technique of selecting the heterostructure materials according to their bulk three-dimensional (3D) lattice properties (specifically, their LO phonon frequencies and the strengths of the corresponding Fröhlich interactions). Reduced dimensionality confers no advantage in phonon band-structure engineering of thermal-equilibrium scattering rates in semiconductor heterostructures.

Finally, we shall mention electron-phonon scattering rates in two cases that are beyond the scope of the rest of this paper. First, non-thermal-equilibrium (e.g., hot-phonon) properties, in contrast to equilibrium properties, can be sensitive to the details of the phonon modes,⁴⁰ since Eqs. (16) and (17) no longer apply. A calculation in the hot-phonon regime must use the correct normal modes of the system. The second case of interest concerns the free-standing semiconductor wafer. In this case, the barriers are free space rather than the similar semiconductors of a heterostructure. It has been suggested⁴¹ that the electron-phonon scattering rates in a free-standing wafer are reduced compared to those in semiconductor QW's. Part of the scattering found in a conventional QW is certainly missing, because the bulklike and interface vibrations of the *barriers* are absent in a free-standing wafer. However, contrary to Ref. 41, the normal modes of the wafer form a set comprising both the bulklike vibrations *and the interface vibrations* of the wafer. If this were not so, the normal modes would not form a complete set (i.e., the interface vibrations of the wafer would have no projection onto *any* mode). The scattering by the interface vibrations of the wafer can be calculated from Eqs. (13) and (19) (see Appendix E) and is stronger than the interface-vibration scattering in a QW because the dielectric constant of the barriers is reduced from its QW value to unity. This enhancement in scattering exceeds the reduction due to the absence of barrier vibrations, except for symmetric vibrations at very small q ,

so that the overall scattering rate is larger in a free-standing wafer than in a semiconductor QW.

ACKNOWLEDGMENTS

The author thanks D. J. Mowbray, A. J. Read, and M. S. Skolnick for critical comments on the manuscript.

APPENDIX A: A FOURTH-ORDER EIGENVALUE EQUATION

This appendix considers the selection of the differential equation (10), and analyzes the properties of the eigenfunctions and eigenvalues of this fourth-order equation. As the first step, we consider the general eigenvalue equation, which can be written as

$$L(\nu) + \lambda P(\nu) = 0, \quad (\text{A1})$$

subject to "standard boundary conditions" (SBC's). SBC's are defined to be the boundary conditions for which the operators L and P are Hermitian. Functionals $\Lambda(\nu)$ and $\Pi(\nu)$ are defined so that for functions $\nu(z)$ that obey SBC's,

$$\Lambda(\nu) = - \int dz \nu^* L(\nu),$$

$$\Pi(\nu) = \int dz \nu^* P(\nu).$$

It is necessary that $\Pi(\nu) \geq 0$ for all $\nu(z)$ that obey SBC's, with equality only if $\nu(z) \equiv 0$. Then the operation

$$\nu_i^* \cdot \nu_j = \int dz \nu_i^* P(\nu_j) \quad (\text{A2})$$

on functions $\nu_i(z)$ and $\nu_j(z)$ that obey SBC's has the algebraic properties of a scalar product.

With these definitions, the properties of the eigenfunctions and eigenvalues of Eq. (A1) can be determined by using the same methods as for second-order Sturm-Liouville equations.⁴² Hence the eigenvalues are real, eigenfunctions with different eigenvalues are orthogonal, eigenfunctions with the same eigenvalue can be orthogonalized by the Gram-Schmidt procedure, and the eigenfunctions form a complete set for functions ψ that obey the same BC's as the eigenfunctions, where the scalar product used in the definitions of orthogonality and completeness is that of Eq. (A2). Also, the eigenproblem arises as the Euler-Lagrange equation both for the variational problem

$$\delta[\Lambda(\nu) - \lambda \Pi(\nu)] = 0$$

subject to SBC's, and for the variational problem $\delta\Lambda(\nu) = 0$ subject to SBC's and the normalization condition $\Pi(\nu) = 1$. If the proofs of these properties are expressed in terms of the quantities L , P , Λ , Π , and the standard boundary conditions, then the algebra of the proofs is identical to that for the Sturm-Liouville problem. The standard proof⁴² of completeness requires, in addition to the SBC's, that the eigenvalues λ have a lower bound but no upper bound.

Let us now consider eigenvalue equations that are suitable for generating the complete orthogonal sets of functions required in Sec. II. For the scalar product (A2) to be the one used in the orthogonality relation (4) that follows from the mechanics, $P(\nu)$ must be given by

$$P(\nu) = - \frac{d^2 \nu}{dz^2} + q^2 \nu. \quad (\text{A3})$$

To satisfy the conditions on the bounds of λ , $L(\nu)$ must be at least fourth order. Equation (10) has the form (A1) with $P(\nu)$ given by (A3) and $L(\nu)$ by

$$L(\nu) = - \frac{d^4 \nu}{dz^4} + q^2 \frac{d^2 \nu}{dz^2}.$$

Hence the SBC's are

$$\nu \nu' = \nu'' \nu = \nu' \nu'' = 0 \quad (\text{A4})$$

at $z=0$ and d . Though the selection of factors ν, ν', ν'', ν''' that vanish at $z=0$ may differ from that at $z=d$, the SBC's further require that at a given boundary the factors that vanish in order to satisfy the SBC's must be the same for all functions $\nu(z)$. As an alternative to (A4), the SBC's may be satisfied with periodic BC's. The three sets of eigenfunctions given in column two of Table I arise when the same BC's are applied at both $z=0$ and $z=d$.

APPENDIX B: COMPLETENESS OF EIGENFUNCTIONS AND RELAXATION OF BOUNDARY CONDITIONS

We consider the expansion in eigenfunctions $\chi_{nq}(z)$ of a function $\psi(z)$ when $\psi(z)$ does not obey the same boundary conditions (BC's) as the $\chi_{nq}(z)$. This extends the proof of completeness discussed in Appendix A, which demands the restriction that $\psi(z)$ must obey these BC's. As in the main text, q is a parameter of the eigenvalue equation and n labels the different eigenfunctions and eigenvalues.

We want to find the circumstances in which the function $\psi(z)$ and its eigenfunction expansion are equal in the sense of Eq. (5), and it is helpful to consider a generalization of this equation. Equation (5) is an example of a relation

$$\lim_{m \rightarrow \infty} (R_m - S_m)^* \cdot (R_m - S_m) = 0, \quad (\text{B1})$$

where $R_m = R_m(z)$ and $S_m = S_m(z)$ are sequences of functions. Equation (B1) expresses an equivalence relation between the sequences R_m and S_m , which we shall denote " \sim ." The equivalence of a sequence to an ordinary function $\psi(z)$ can be expressed by defining the sequence F_m so that $F_m = \psi$ for all m . When the sequences R_m and S_m are defined for each value of a parameter σ , the definition of equivalence can be extended to include the notion of a limit. Thus the statement

$$\lim_{\sigma \rightarrow \tau} R(z; \sigma) \sim \lim_{\sigma \rightarrow \tau} S(z; \sigma)$$

means that

$$\lim_{\sigma \rightarrow \tau} \lim_{m \rightarrow \infty} (R_m - S_m)^* \cdot (R_m - S_m) = 0.$$

Our problem is to find out whether functions $\psi(z)$ that do not obey the same BC's as $\chi_{nq}(z)$ nevertheless satisfy

$$\psi(z) \sim \sum_n c_n \chi_{nq}(z), \quad (\text{B2})$$

where $c_n = \chi_{nq}^* \cdot \psi / \chi_{nq}^* \cdot \chi_{nq}$.

The method of relaxing the BC's on $\psi(z)$, when this is possible, is to introduce a function $\psi(z, z_0) = \psi(z) - g(z, z_0)$, which does obey the necessary BC's, and show that

$$\begin{aligned} \psi(z) &\sim \lim_{z_0 \rightarrow 0} \check{\psi}(z, z_0) \sim \lim_{z_0 \rightarrow 0} \sum_n \check{c}_n(z_0) \chi_{nq}(z) \\ &\sim \sum_n c_n \chi_{nq}(z), \end{aligned} \quad (\text{B3})$$

where $\check{c}_n = \chi_{nq}^* \check{\psi} / \chi_{nq}^* \chi_{nq}$. Since $\check{\psi}(z)$ obeys the same BC's as the $\chi_{nq}(z)$, the second equivalence in Eq. (B3) is simply Eq. (5), the proof of which is discussed in Appendix A. The first and third equivalences in Eq. (B3) require that

$$\lim_{z_0 \rightarrow 0} g^* \cdot g = 0. \quad (\text{B4})$$

Thus $g(z, z_0)$ must satisfy two conditions: for each z_0 it ensures that $\check{\psi}$ satisfies the correct BC's at $z=0$ and d ; and its norm must vanish in the limit as $z_0 \rightarrow 0$.

To enforce BC's $\check{\psi}'(0)=0$, $\check{\psi}''(0)=0$, and $\check{\psi}'''(0)=0$ when the dot product is defined by Eq. (4), suitable functions $g(z, z_0)$ are

$$g(z, z_0) = -\psi'(0)z \left[1 - \frac{z^2}{2z_0^2} \right] \exp(-z/z_0)h(z/d), \quad (\text{B5})$$

$$g(z, z_0) = -\psi''(0) \frac{z^2}{2} \exp(-z/z_0)h(z/d), \quad (\text{B6})$$

and

$$g(z, z_0) = -\psi'''(0) \frac{z^3}{6} \exp(-z/z_0)h(z/d), \quad (\text{B7})$$

respectively. The function $h(t)$ has $h(0)=1$, $h(1)=0$, and its first, second, and third derivatives vanish both at $t=0$ and $t=1$. The purpose of the factor $h(z/d)$ in Eqs. (B5)–(B7) is to make the enforcement of the BC's at $z=0$ and d mutually independent. A suitable $h(t)$ is the polynomial

$$h(t) = (1-t)^4(1+4t)(1+10t^2)(1-20t^3).$$

The BC's $\check{\psi}'(d)=0$, $\check{\psi}''(d)=0$, and $\check{\psi}'''(d)=0$ can similarly be enforced with functions $g(z, z_0)$ given by Eqs. (B5)–(B7), respectively, after making the following substitutions in these equations: $z \rightarrow d-z$, $\psi'(0) \rightarrow -\psi'(d)$, $\psi''(0) \rightarrow \psi''(d)$, and $\psi'''(0) \rightarrow -\psi'''(d)$. To enforce one of the combinations of BC's given in column three of Table I, the appropriate $g(z, z_0)$ is simply the sum of the expressions given for the individual BC's. By applying the Schwarz inequality, it can be seen that this sum obeys the condition (B4).

The fact that suitable $g(z, z_0)$ exist for the BC's discussed above means that each equivalence in Eq. (B3) is valid, and so Eq. (B2) follows even though the derivatives of $\psi(z)$ do not obey the same BC's as the $\chi_{nq}(z)$. However, the BC's $\check{\psi}(0)=0$ and $\check{\psi}(d)=0$ cannot be enforced in this way when the dot product is defined by Eq. (4), since no $g(z, z_0)$ satisfying Eq. (B4) exist for these cases. This is not surprising, since (in the terminology of the main text) when $\chi_{nq}(0)=\chi_{nq}(d)=0$, the eigenfunctions $\chi_{nq}(z)$ comprise the bulklike vibrations only, and a function with $\psi(0) \neq 0$ or $\psi(d) \neq 0$ has a projection onto the interface vibrations, which are orthogonal to the bulklike vibrations (see Sec. II).

APPENDIX C: UNITARY TRANSFORMATIONS BETWEEN DIFFERENT BASIS SETS

If a set of basis functions \hat{u}_m (with the caret denoting normalization) is orthonormal and complete, then an arbitrary function f can be written as

$$f \sim \sum_m a_m \hat{u}_m,$$

where $a_m = \hat{u}_m^* \cdot f$ and the equivalence relation is discussed in Appendix B. Similarly, for a second basis set \hat{v}_n that is orthonormal and complete,

$$f \sim \sum_n b_n \hat{v}_n,$$

where $b_n = \hat{v}_n^* \cdot f$. The a_m and b_n are vector representations of the function f and are related by the transformation U_{nm} , where

$$a_m = \sum_n U_{nm} b_n.$$

It follows from the orthonormality and completeness of the basis functions \hat{u}_m and \hat{v}_n that

$$U_{nm} = \hat{u}_m^* \cdot \hat{v}_n, \quad (\text{C1})$$

$$b_n = \sum_m U_{nm}^* a_m, \quad (\text{C2})$$

and that U_{nm} has the unitary property

$$\sum_n U_{nm}^* U_{nm'} = \delta_{mm'}, \quad (\text{C3a})$$

$$\sum_m U_{nm}^* U_{n'm} = \delta_{nn'}. \quad (\text{C3b})$$

If the u_m and v_n are unnormalized basis functions, then $\hat{u}_m = u_m / (u_m^* \cdot u_m)^{1/2}$, $\hat{v}_n = v_n / (v_n^* \cdot v_n)^{1/2}$, and Eq. (C1) becomes

$$U_{nm} = \frac{u_m^* \cdot v_n}{(u_m^* \cdot u_m)^{1/2} (v_n^* \cdot v_n)^{1/2}}. \quad (\text{C4})$$

Now let the v_n be the slab vibrations of Table I, and the u_m be the reformulated slab vibrations of Table I and Eq. (9) [but with m in place of the label n used in Table I and Eq. (9), and with the same value of q as for the slab vibrations]. It is shown in Sec. II that the u_m and the v_n each form a complete set for the bulklike vibrations of a layer. It follows from Eq. (C4) that U_{nm} is given by

$$U_{nm} = 0 \quad (\text{C5a})$$

if $m+n$ is odd,

$$\begin{aligned} U_{nm} = & \frac{4}{\pi} \frac{n+1}{\mu_{mq}^2 - (n+1)^2} \frac{[q^2 d^2 + \mu_{mq}^2 \pi^2]^{1/2}}{[q^2 d^2 + (n+1)^2 \pi^2]^{1/2}} \\ & \times \frac{\sin \frac{1}{2} \mu_{mq} \pi}{\left[1 - \frac{1}{\mu_{mq} \pi} \sin \mu_{mq} \pi \right]^{1/2}} \end{aligned} \quad (\text{C5b})$$

if m and n are both odd, and

$$U_{nm} = -\frac{4}{\pi} \frac{n+1}{\mu_{mq}^2 - (n+1)^2} \frac{[q^2 d^2 + \mu_{mq}^2 \pi^2]^{1/2}}{[q^2 d^2 + (n+1)^2 \pi^2]^{1/2}} \times \frac{\cos \frac{1}{2} \mu_{mq} \pi}{\left[1 + \frac{1}{\mu_{mq} \pi} \sin \mu_{mq} \pi\right]^{1/2}} \quad (\text{C5c})$$

if m and n are both even. The interface vibrations are orthogonal to all the bulklike vibrations and are not affected by this transformation.

Now let v_n for $n \geq 0$ be the slab vibrations, v_n for $n = \bar{1}$ and $\bar{2}$ be the interface vibrations (as defined in Sec. II), and u_m be the guided vibrations of Table I (with m in place of the label n used in Table I, and with the same value of q as for the slab vibrations and interface vibrations). Section II shows that the u_m and the v_n each form a complete set for all the vibrations of a layer. U_{nm} is given by

$$U_{nm} = 0 \quad (\text{C6a})$$

if $m+n$ is odd,

$$U_{nm} = \frac{2}{\pi} \frac{B_m}{[q^2 d^2 + m^2 \pi^2]^{1/2} [q^2 d^2 + (n+1)^2 \pi^2]^{1/2}} \times \left[\frac{q^2 d^2 - (n+1)m \pi^2}{n+1+m} + \frac{q^2 d^2 + (n+1)m \pi^2}{n+1-m} \right] \quad (\text{C6b})$$

if $m+n$ is even and $n \geq 0$,

$$U_{\bar{1}m} = - \left[\frac{4qd}{q^2 d^2 + m^2 \pi^2} \coth \frac{1}{2} qd \right]^{1/2} \quad (\text{C6c})$$

if m is odd, and

$$U_{\bar{2}m} = B_m \left[\frac{4qd}{q^2 d^2 + m^2 \pi^2} \tanh \frac{1}{2} qd \right]^{1/2} \quad (\text{C6d})$$

if m is even, where $B_m = 1$ if $m \neq 0$ and $2^{-1/2}$ if $m = 0$.

The unitary property (C3) has been verified numerically both for the transformation given by Eq. (C5) and for that given by Eq. (C6).

APPENDIX D: TRANSVERSE-OPTIC MODES AND RETARDATION

1. Introduction

The main text of the present work gives a nonretarded (electrostatic) treatment of the electromagnetic field. A full treatment of the phonon modes must include both electromagnetic retardation³⁵ and bulk phonon dispersion, for example by adding terms in the magnetic vector potential \mathbf{A} to Eq. (21), to give

$$\mathcal{L} = \frac{1}{2} \frac{\partial \mathbf{w}}{\partial t} \cdot \frac{\partial \mathbf{w}}{\partial t} - \frac{1}{2} \omega_T^2 \mathbf{w} \cdot \mathbf{w} + \frac{1}{2} \epsilon_0 \epsilon(z; \infty) \mathbf{E} \cdot \mathbf{E} + \gamma \mathbf{w} \cdot \mathbf{E} - \frac{1}{2} \frac{1}{\mu_0} \mathbf{B} \cdot \mathbf{B} + \frac{1}{2} \sum_{ijkl} Z_{ijkl} \frac{\partial w_k}{\partial r_j} \frac{\partial w_l}{\partial r_i},$$

where $\mathbf{E} = -\nabla\Phi - \partial \mathbf{A}/\partial t$ and $\mathbf{B} = \nabla \times \mathbf{A}$. Appendix D 3 investigates the effects of retardation on the properties of the LO modes discussed in the main text. Retardation is likely to be significant for the TO modes, particularly for the transverse electric (TE) polarization, but a full treatment of the TO modes is beyond the scope of this paper. However, the TO modes of the nonretarded theory will be discussed in Appendix D 2 to provide results for use in the main text.

Note that a polariton theory that does not include bulk phonon dispersion gives a quite different description of the TO modes, even at large q . However, this description is not appropriate for III-V semiconductor heterostructures where the bulk phonon dispersion cannot be neglected. The inclusion of bulk phonon dispersion introduces additional TE and transverse magnetic (TM) solutions in the polariton complex band structure, and these solutions must be included in the matching procedure that determines the normal modes. Some of the TM polaritons correspond in the nonretarded limit to the interface vibrations of the present work (see Appendix D 3).

2. TO modes in the electrostatic theory

The treatment of TO modes corresponds closely to that of LO modes. One can identify orthogonal complete sets of vibrations, normal modes of a slab subject to boundary conditions, and normal modes of a heterostructure with connection rules derived from the Euler-Lagrange equations.

The different phonon polarizations in this isotropic theory can be found by examination of the equations of motion. It follows from Eqs. (22) and (23) and the translational invariance of the slab in the x - y plane that \mathbf{w} is a linear combination of solutions of the form $\mathbf{w} = \mathbf{w}_0(z) \exp(iqx)$, where, without loss of generality, the direction of the x axis is chosen to be parallel to \mathbf{q} . Equations (22) and (23) also show that the motion involving w_y (the TE polarization²⁹) is independent of that involving w_x and w_z (the LO and TM polarizations²⁹). Within a single layer, the LO solutions obey $\mathbf{w} = -\nabla\chi$ (i.e., $\nabla \times \mathbf{w} = 0$) and are discussed in the main text. Within a single layer, the TO (TE and TM) solutions obey $\mathbf{w} = \nabla \times \mathbf{S}$ (i.e., $\nabla \cdot \mathbf{w} = 0$) and will be discussed here. The interface vibrations can be classified both as LO and as TM, as will be shown below.

For the TE polarization, the Euler-Lagrange equations simplify to

$$\frac{\partial^2 w_y}{\partial t^2} + \omega_T^2 w_y + A \nabla^2 w_y = 0, \quad (\text{D1})$$

$$\Phi = 0.$$

Equation (D1) is second order and has SBC's $w_y, w_y' = 0$ at $z = 0$ and d . Equation (D1) serves both to generate complete sets of TE vibrations and as the Euler-Lagrange equation for the TE modes, and so the SBC's are the same for both purposes. The solutions that obey the same BC's at both $z = 0$ and $z = d$ are

$$w_y = \xi(z) \exp(iqx), \quad (\text{D2})$$

where

$$\xi = \sin \frac{(n+1)\pi z}{d}, \quad n=0,1,2,\dots, \quad (\text{D3})$$

$$\xi = \cos \frac{n\pi z}{d}, \quad n=0,1,2,\dots, \quad (\text{D4})$$

and the BC's are $\xi(0)=\xi(d)=0$, $\xi'(0)=\xi'(d)=0$, respectively. Each set of vibrations corresponds to the normal modes for the motion of the slab constrained by these BC's. Substitution of Eq. (D2) into the general orthogonality relation (1) shows that the orthogonality and completeness relations for TE vibrations are governed by the dot product

$$\xi_\mu^* \cdot \xi_\nu = \frac{1}{2d} \int_0^d dz \xi_\mu^*(z) \xi_\nu(z).$$

Hence each set of TE vibrations (D3) and (D4) is complete.

For the TE modes of a layer in a heterostructure in the limit of infinitesimal dispersion, there are no slowly varying components outside the layer, and so the connection rule derived in Sec. VI C, that $\rho^{-1/2}w_y$ is continuous, reduces to boundary conditions $w_y=0$ at $z=0$ and d . Hence the normal modes are given by Eq. (D3).

For the TM polarization it is very useful to introduce a mechanical vector potential for \mathbf{w} . Within a slab, the solutions of the Euler-Lagrange equations (22) and (23) that have the form $\mathbf{w}=\nabla\times\mathbf{S}$ obey

$$\nabla\times\nabla\times[(\omega_T^2-\omega^2)\mathbf{S}+A\nabla^2\mathbf{S}]=0, \quad (\text{D5})$$

$$\nabla\Phi = -\frac{1}{\gamma}\nabla\times[(\omega_T^2-\omega^2)\mathbf{S}+A\nabla^2\mathbf{S}]. \quad (\text{D6})$$

If the gauge $\nabla\cdot\mathbf{S}=0$ is chosen, then (D5) becomes

$$(\omega_T^2-\omega^2)\nabla^2\mathbf{S}+A\nabla^2\nabla^2\mathbf{S}=0. \quad (\text{D7})$$

Without loss of generality, the gauge for the TM polarization ($w_y=0$) can be chosen so that

$$\mathbf{S} = \begin{pmatrix} 0 \\ 1 \\ 0 \end{pmatrix} \bar{\xi}(x,z), \quad (\text{D8})$$

where $\bar{\xi}(x,z)=\xi(z)\exp(iqx)$. Then \mathbf{w} is related to ξ by

$$\mathbf{w} = \begin{pmatrix} -\frac{\partial}{\partial z}\xi \\ 0 \\ iq\xi \end{pmatrix} \exp(iqx),$$

and so the general orthogonality relation (1) leads to definitions of orthogonality and completeness based on the dot product

$$\xi_\mu^* \cdot \xi_\nu = \frac{1}{2d} \int_0^d dz q^2 \xi_\mu^*(z) \xi_\nu(z) + \frac{d\xi_\mu^*}{dz} \frac{d\xi_\nu}{dz}. \quad (\text{D9})$$

Within a single layer, the interface vibrations defined in Sec. II obey $\mathbf{w}=-\nabla\bar{\chi}$, $\nabla^2\bar{\chi}=0$. Thus they obey $\nabla\cdot\mathbf{w}=0$ and so they can also be represented by $\mathbf{w}=\nabla\times\mathbf{S}$. It fol-

lows that the interface vibrations can be classified both as LO vibrations ($\mathbf{w}=-\nabla\bar{\chi}$) and as TM vibrations ($\mathbf{w}=\nabla\times\mathbf{S}$). The property $\mathbf{w}=-\nabla\bar{\chi}$ implies that $\nabla\times\mathbf{w}=0$ and so \mathbf{S} obeys $\nabla\times\nabla\times\mathbf{S}=0$. If the gauge $\nabla\cdot\mathbf{S}=0$ is chosen, the equation for \mathbf{S} becomes $\nabla^2\mathbf{S}=0$. It follows from this result that the interface vibrations satisfy the equation (D7) for TM vibrations, as well as the equation (24) for LO vibrations. It is not surprising that the interface vibrations are solutions both of the equation for vibrations of the form $\mathbf{w}=-\nabla\bar{\chi}$ and of the equation for vibrations of the form $\mathbf{w}=\nabla\times\mathbf{S}$, since the interface vibrations satisfy both these conditions.

The TM vibrations are readily calculated with the choice of gauge (D8). With this gauge, the interface vibrations obey $\nabla^2\bar{\xi}=0$. Hence $\bar{\xi}$ for interface vibrations is a linear combination of $\exp(qz)$ and $\exp(-qz)$. The conditions for orthogonality to interface vibrations are $\bar{\xi}(0)=\bar{\xi}(d)=0$. Vibrations that satisfy these conditions are termed bulklike TM vibrations (cf. bulklike LO vibrations). Substituting the choice of gauge (D8) into Eq. (D7), one finds

$$(\omega_T^2-\omega^2)\nabla^2\bar{\xi}+A\nabla^2\nabla^2\bar{\xi}=0. \quad (\text{D10})$$

Equations (D9) and (D10) have the same form as (4) and (24), respectively, but with ξ in the role of χ .

Thus complete sets of TM vibrations can be found from Table I by replacing χ with ξ . Note that ξ and \mathbf{w} have opposite parity, so that in Table I symmetric TM vibrations have odd n , and antisymmetric TM vibrations have even n . Equations (30) and (31), the SBC's on \mathbf{w} for the Euler-Lagrange equations for a slab, reduce to $\xi'=0$ and $\xi'\xi''=\xi=0$, respectively. Thus either $\xi'=0$ or $\xi=\xi''=0$. Also Φ must obey both Poisson's equation (23) beyond the slab and the SBC (29). The normal modes that obey the BC $\xi'=0$ in general correspond neither to the reformulated slab vibrations nor to the guided vibrations. However, as $q\rightarrow 0$, the modes with $\omega\approx\omega_T$ tend towards the guided vibrations with $n\neq 0$, and as $A\rightarrow 0$ (infinitesimal dispersion) the $q\neq 0$ modes tend towards the reformulated slab vibrations with $\Phi=0$. The modes that obey the BC's $\xi=\xi''=0$ are the slab vibrations and have $\Phi=0$. The guided vibrations with $\Phi=0$ obey the Euler-Lagrange equations within the slab but do not obey Eq. (29) except in the case $q=0$: the guided-vibration BC's $\xi'=\xi'''=0$ are not compatible with the SBC $\varphi(\pm\infty)\varphi'(\pm\infty)=0$ except in the case $q=0$. Thus the conclusions about the different complete sets of vibrations, and about the normal modes of a slab subject to BC's, are the same for TM as for LO vibrations.

To find the TM normal modes of a slab in a heterostructure in the limit of infinitesimal dispersion, one should apply the connection rules found in Sec. VI C, i.e., the continuity of Φ , D_z , and $\rho^{-1/2}w_x$. The antisymmetric TM modes have a simple behavior, their dispersion being that of even-numbered reformulated slab vibrations, Eq. (37). The symmetric TM modes are more complicated, since the bulklike TM vibrations interact with the symmetric interface mode, and the dispersion is governed by Eq. (36) but with the factor $-N\mu$ replaced by XA , where

$$X = \frac{\epsilon_1(\infty)(\omega_{L1}^2 - \omega_{T2}^2)}{\epsilon_2(\infty)(\omega_{L2}^2 - \omega_{T2}^2)(\omega_{T1}^2 - \omega_{T2}^2)}.$$

The symmetric modes at $q=0$ are the guided vibrations with $n=1,3,5,\dots$. As q increases the modes evolve from the $n=3,5,7,\dots$ guided vibrations into the $n=1,3,5,7,\dots$ reformulated slab vibrations, and from the $n=1$ guided vibration into the symmetric interface mode. At $q \sim k$ the dispersion of the reformulated slab vibrations changes in a manner similar to that for LO modes (Fig. 4). If the bulk dispersion A were negative, the symmetric interface mode would cross and interact strongly with the bulklike TM modes at small q . This behavior is similar to that of antisymmetric LO modes because both the symmetric TM and the antisymmetric LO modes are governed by an equation of the form (36).

3. Effects of retardation

The nonretarded and retarded theories agree for heterostructures if the following hold: (1) the connection rules at an interface are the same; (2) at each (\mathbf{q}, ω) the bulk solutions of the two theories for complex k are in one-to-one correspondence. The corresponding solutions must also have the same field distributions, at least for the fields that are involved in the connection rules. (3) The scattering rates for electrons are the same, taking all fields into account. When these three conditions are satisfied, the modes of a heterostructure have the same frequencies and scattering rates in the two theories. The following paragraphs determine the circumstances in which these conditions are met.

The connection rules in a retarded theory can be obtained by analysis similar to that of Sec. VI, but using the Lagrangian density given in Appendix D 1. Thus in the retarded theory the connection rules are the continuity of the mechanical fields \mathbf{u} and \mathbf{u}' and the electromagnetic fields E_x, E_y, D_z, H_x, H_y , and B_z , where \mathbf{E} is the electric field, \mathbf{D} is the electric displacement, \mathbf{B} is the magnetic induction, and \mathbf{H} is the magnetic intensity, which is equal to \mathbf{B}/μ_0 in nonmagnetic materials. The connection rules in the retarded and nonretarded theories are most easily compared by discussing the TM and LO modes separately from the TE modes. For the TM and LO polarized modes of interest in the present work, u_y, u'_y, E_y, H_x , and B_z vanish everywhere, and the condition on H_y is equivalent to that on D_z . Thus the conditions on the electromagnetic fields can be expressed as the continuity of E_x and D_z only. In the nonretarded theory (Sec. VI) the fields $\mathbf{u}, \mathbf{u}', \Phi$, and D_z are continuous, and $\mathbf{E} = -\nabla\Phi$, so the continuity of Φ is equivalent to the continuity of E_x . Hence the connection rules in the retarded theory are the same as those in the nonretarded theory.

The correspondence between the complex band structure of the bulk in the retarded and nonretarded theories is evident from Fig. 5. This figure plots the complex dispersion relations in the retarded theory for LO waves [Eq. (28)] and for TM waves, the latter given by

$$K^2 = \epsilon_T(K, \omega)\omega^2/c^2, \quad (\text{D11})$$

where $\epsilon_T(K, \omega)$ is the transverse dielectric function

$$\epsilon_T(K, \omega) = \epsilon(\infty) \left[1 + \frac{\omega_L^2 - \omega_T^2}{\omega_T^2 - \omega^2 - AK^2} \right],$$

and the experimental value²⁸ of A for $\mathbf{K} \parallel [001]$ is

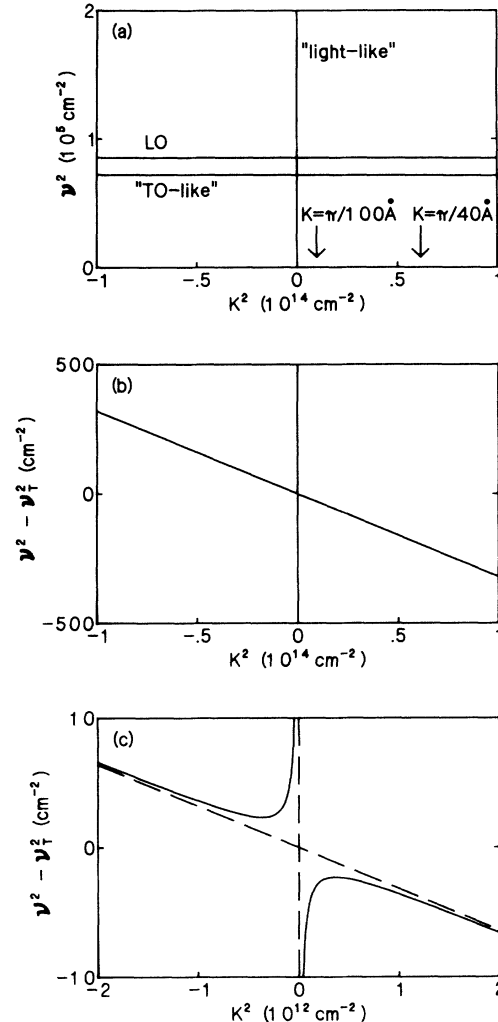


FIG. 5. Complex band structure for optic phonons of GaAs near the zone center, including retardation. The plot of frequency squared (ν^2) against wave vector squared (K^2) facilitates comparison with the nonretarded theory, since the dispersion curves of the latter are straight lines when plotted in this way. (a) On these scales the dispersion and the differences from the nonretarded theory are not evident. The arrows indicate the wave vector π/d for $d=40$ and 100 Å. (b) Frequency scale expanded about the TO frequency ν_T , with range approximately $\nu_T \pm 0.93$ cm^{-1} . Here the dispersion of the TO phonons is clear, but the differences from the nonretarded theory are still not obvious. (c) Expanded wave-vector and frequency scales show differences between the retarded theory (solid lines) and the nonretarded theory (dashed lines). The vertical dashed line corresponds to the interface vibrations of the nonretarded theory, the other dashed line to the TM vibrations of the nonretarded theory. The frequency range is now $\nu_T \pm 0.019$ cm^{-1} and the wave-vector range is smaller than in (a) and (b). The LO dispersion curve, off scale in (b) and (c), is a (sloping) straight line, and is the same in the retarded and the nonretarded theories.

$3.2 \times 10^{-12} (2\pi c)^2$. At each (\mathbf{q}, ω) the retarded and nonretarded theories each have two LO and four TM solutions [each value of K^2 gives a pair of solutions $\pm K$; in the gap for $|\nu^2 - \nu_T^2| < 2.3 \text{ cm}^{-2}$ in Fig. 5(c), K^2 is complex and is not plotted]. Over most of the frequency range (away from ω_T , but including frequencies close to ω_L), Eq. (D11) has solutions with small K (Fig. 5). These solutions correspond to the interface vibrations of the nonretarded theory, which have $K=0$. The retarded theory has another pair of TM solutions (at larger K) which correspond closely to the TM solutions of the nonretarded theory. The agreement between the two theories is exact for the LO solutions.

We now compare the fields for the small- K TM waves of the retarded theory and the interface vibrations of the nonretarded theory. Consider the symmetric TM vibration with electric field

$$\mathbf{E} = - \begin{pmatrix} i\kappa \cosh \kappa z' \\ 0 \\ q \sinh \kappa z' \end{pmatrix} \exp(iqx - i\omega t) \quad (\text{D12})$$

in which $z'=0$ is the symmetry plane. $q^2 - \kappa^2 = K^2$ and K is related to ω by the dispersion relation (D11). The solutions of most importance for the scattering of electrons have $q^2 \gg q^2 - \kappa^2$. Thus the electric field \mathbf{E} is very close to

$$\mathbf{E} = - \begin{pmatrix} iq \cosh qz' \\ 0 \\ q \sinh qz' \end{pmatrix} \exp(iqx - i\omega t) \quad (\text{D13})$$

and it tends towards this expression in the nonretarded ($c \rightarrow \infty$) limit. But Eq. (D13) is that of the symmetric interface vibration in the nonretarded theory. The exact electric field (D12) can be written as

$$\mathbf{E} = -\nabla\Phi - \frac{\partial \mathbf{A}}{\partial t}, \quad (\text{D14})$$

where Φ is the electrostatic potential for a nonretarded interface vibration, and \mathbf{A} is a residual vector potential of order $1/c^2$. In this way, the small- K TM waves tend to the interface vibrations of the nonretarded treatment as $c \rightarrow \infty$. It is also notable that for fixed q , a change in ω gives rise to a negligible change (of order $1/c^2$) in κ . This corresponds to the property, in the nonretarded treatment, that the functional form of the interface vibrations is independent of frequency (Sec. VI A). In summary, the nonretarded solutions are a good approximation to the retarded solutions as long as both (A) the retarded theory has solutions with small K , i.e., ω is not very close to ω_T (Fig. 5), and (B) q is not too small, i.e., the condition $q^2 \gg K^2$ is satisfied.

We now examine the fields for the other solutions of the bulk problem. The LO solutions are identical in the retarded and nonretarded theories. For the TM solutions with large K , the nonretarded theory sets $\mathbf{E}=\mathbf{B}=\mathbf{0}$ and so does not give the same fields as the retarded theory. This may lead to inaccuracies in the treatment of the TM modes. However, the rapidly varying (large k) TM vibrations that contribute to the LO modes (Sec. VI C) are accurately treated because the large k value makes the electromagnetic fields for these vibrations in a retarded theory very weak compared to the fields of the LO and

small- K TM vibrations.

Electrons are scattered both by the scalar potential Φ and by the vector potential \mathbf{A} of Eq. (D14). The scattering rate is invariant under gauge transformations. As noted above, when Φ is chosen to be the scalar potential for the nonretarded interface vibration, \mathbf{A} is negligible if the conditions (A) and (B) are met.

Thus the conditions (1)–(3) above are satisfied for the LO modes as long as both (A) ω is not very close to ω_T and (B) q is large compared to K . For the LO modes of interest here, condition (A) is satisfied. Condition (B) indicates that the nonretarded theory breaks down at very small values of q , close to the light line. For $q < q_0$ where $q_0 = [\epsilon_{T1}(\omega_{L2})]^{1/2} \omega_{L2}/c = 6894 \text{ cm}^{-1}$, the modes with ω close to ω_{L2} are no longer confined to the GaAs because the small- K TM vibrations of the AIAs are oscillatory rather than evanescent. The GaAs-like LO modes are resonances in the AIAs lightlike polariton continuum. Dispersion curves for the GaAs-like LO modes are strictly defined only for $q > q_0$. It is possible to extend these curves to $q < q_0$, however, by plotting the condition for a resonant mode, i.e., for the AIAs continuum vibrations to have a large amplitude in the GaAs. This approach will be used below.

The modes with $\omega \approx \omega_{L2}$ can be calculated in a retarded theory by a method analogous to that applied in Sec. VID in the absence of retardation. The distinction between slowly varying and rapidly varying vibrations (Sec. VIC), and the effects of the latter at $\omega \approx \omega_{L2}$ are the same in the retarded and nonretarded theories. Thus when the approximation of weak dispersion is valid, the normal modes can be found by matching the slowly varying vibrations, using the connection rules that E_x , D_z , and u_z are continuous. Figure 3 presents the results of a nonretarded calculation with reduced dispersion and the approximation of Eq. (35) (Sec. VID). The experimental value of the GaAs dispersion can be used, but the results are then less accurate because, as discussed in Sec. VID, the approximation (35) is not as good. A nonretarded calculation for a 100-Å GaAs/AIAs QW using the same approximation, but with the experimental value of dispersion, shows the same features as Fig. 3 but on a scale of qd from 0 to 0.4. When retardation is included, the results are again similar [Fig. 6(a)], except for $qd < 0.01$ where the modes have additional dispersive features [Fig. 6(b)]. These features can be interpreted as interactions with the antisymmetric interface modes calculated in a retarded theory with $\mu = A = 0$ (in the same way that the dispersion of Fig. 3 is interpreted in Sec. VID as interactions with interface modes). These additional features will be very difficult to observe in Raman scattering because (a) they are very strongly dispersive, and (b) they occupy a very small area of q space, and so their integrated scattering strength is small. The latter reason (b) also implies that these features are entirely negligible in calculations of electron-phonon-scattering rates.

In conclusion, a nonretarded theory is perfectly adequate for calculations of scattering rates by polar-optic phonons. It does not agree with the full retarded theory at very small q (close to the light line), but these discrepancies have a negligible effect on electron-phonon

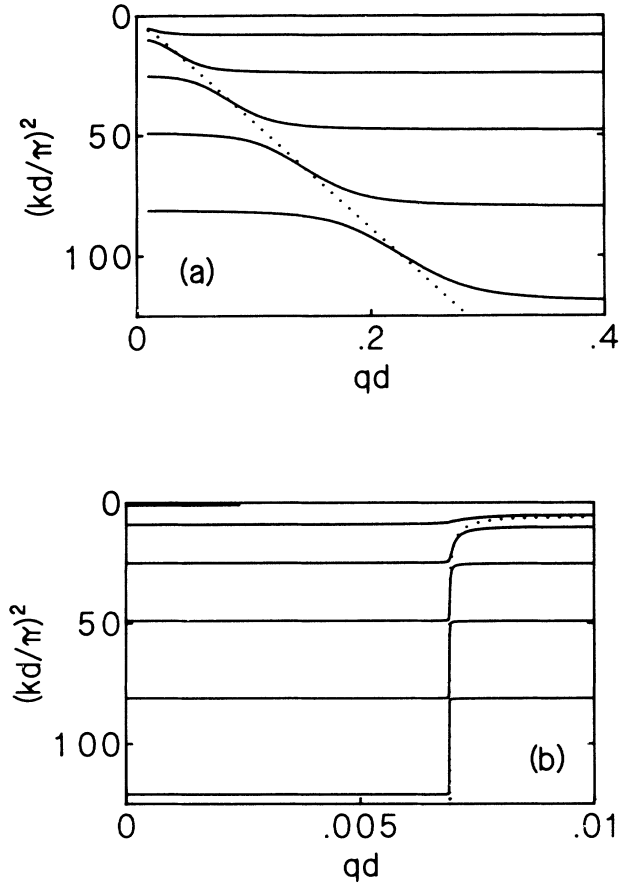


FIG. 6. Solid lines are dispersion curves of antisymmetric GaAs-like LO modes in a 100-Å GaAs/AlAs QW, calculated in a retarded theory. The experimental value of the dispersion was used, with the approximations of Sec. VI D. $(kd/\pi)^2$ is plotted on the y axis, as in Figs. 3 and 4. The dotted line is the antisymmetric GaAs-like interface mode calculated with retardation but without bulk dispersion (i.e., $\mu = A = 0$). (a) For $qd > 0.01$ the dispersion curves are very similar to those calculated without retardation (see text and Fig. 3). (b) For $qd < 0.01$ there are dispersive features, which do not occur in the nonretarded theory. These can be interpreted as interactions with the interface mode (dotted line). The latter occurs at values of qd slightly larger than those for the AlAs light line, which is given approximately on this scale by $qd = q_0 d$, where $q_0 d = 0.006894$. For $qd < q_0 d$ the modes plotted are resonances in the continuum of AlAs lightlike polaritons (see text). The uppermost resonance, at $kd/\pi \approx 1$, broadens and weakens with increasing q , losing its identity at $q \approx 0.38q_0$. In narrower QW's (in which the different LO modes can be resolved by Raman scattering) the uppermost resonant mode is well defined over a wider range of q , up to $q \approx 0.995q_0$ in a 25-Å QW. The second resonant mode becomes the uppermost mode at $q > q_0$. In a 25-Å QW this mode crosses the interface-mode dispersion curve and kd/π achieves a minimum value of 1.04. Thus, as for the lower modes in a 100-Å QW, the interaction with the steeply rising interface mode causes only a small interruption in the much flatter dispersion of the LO modes.

scattering and may not be observable even in Raman scattering.

APPENDIX E: INTERFACE VIBRATIONS OF A FREE-STANDING WAFER

The electron-phonon-scattering potential for the interface vibrations of a polar layer can be found by solution of Eq. (13). The results for the case where $\epsilon(z; \infty)$ is independent of z are those given in Table I and discussed in Secs. III and IV. These potentials can be used to calculate the form factors defined by Eq. (19) for the case of scattering by interface vibrations. Thus the form factor for intrasubband scattering of perfectly confined electrons in the lowest subband is

$$f_{\bar{2}}(q) = 4 \sinh^2 \frac{qd}{2} \tanh \frac{qd}{2} \exp(-qd) \times \left[\frac{1}{qd} - \frac{qd}{(qd)^2 + 4\pi^2} \right]^2, \quad (\text{E1})$$

and the form factor for intersubband scattering of perfectly confined electrons between the lowest two subbands is

$$f_{\bar{1}}(q) = 4 \cosh^2 \frac{qd}{2} \coth \frac{qd}{2} \exp(-qd) \times \left[\frac{qd}{(qd)^2 + \pi^2} - \frac{qd}{(qd)^2 + 9\pi^2} \right]^2. \quad (\text{E2})$$

These results are plotted as f^I in Figs. 1(d) and 2(d), respectively.

The method is similar when $\epsilon(z; \infty)$ is not independent of z . When $\epsilon(z; \infty)$ is equal to $\epsilon_1(\infty)$ in the barriers and $\epsilon_2(\infty)$ in the layer, the potentials within the layer are equal to those of Table I multiplied by

$$T_{\bar{2}} = \exp \frac{qd}{2} \left[\frac{\epsilon_1(\infty)}{\epsilon_2(\infty)} \cosh \frac{qd}{2} + \sinh \frac{qd}{2} \right]^{-1},$$

$$T_{\bar{1}} = \exp \frac{qd}{2} \left[\frac{\epsilon_1(\infty)}{\epsilon_2(\infty)} \sinh \frac{qd}{2} + \cosh \frac{qd}{2} \right]^{-1}$$

for symmetric and antisymmetric vibrations, respectively. The form factors $f_{\bar{2}}(q)$ and $f_{\bar{1}}(q)$ are those of Eqs. (E1) and (E2) multiplied by $(T_{\bar{2}})^2$ and $(T_{\bar{1}})^2$, respectively.

The interface vibrations of the barriers in a QW structure are defined by

$$\chi = \exp -q(z - d/2), \quad z > d,$$

$$\chi = \pm \exp +q(z - d/2), \quad z < 0,$$

with the positive and negative signs for symmetric and antisymmetric vibrations, respectively, and with $\mathbf{w} = 0$ for $0 < z < d$. The form factors for scattering of electrons by these vibrations can be found from Eqs. (19) and (13) [the latter modified for barrier vibrations by changing the sign of η and by using barrier values of $\epsilon(\infty)$ and β]. It is found that the form factor for intrasubband scattering by symmetric vibrations is equal to that of Eq. (E1) multiplied by

$$\left[\frac{\epsilon_1(\infty)}{\epsilon_2(\infty)} T_2 \right]^2 \coth \frac{qd}{2},$$

while the form factor for intersubband scattering by antisymmetric vibrations is equal to that of Eq. (E2) multiplied by

$$\left[\frac{\epsilon_1(\infty)}{\epsilon_2(\infty)} T_1 \right]^2 \tanh \frac{qd}{2}.$$

The scattering by bulklike vibrations of the GaAs layer is the same, whether the layer is clad by AlAs barriers or is free standing. If the electrons are taken to be perfectly confined to the GaAs, then they are not scattered by the bulklike vibrations of the AlAs barriers.

An exact comparison of scattering rates in systems with a range of phonon frequencies should find the normal modes and use Eqs. (16) and (17). This is difficult because, in contrast to the semiconductor heterostructure treated in Sec. VI B, it is not clear what surface terms should be included in the Lagrangian density, or what BC's to apply at the surfaces, without recourse to microscopic theory. Fortunately, a good approximation to the scattering rates can be obtained, as discussed in Sec. VII, without knowing the normal modes. The scattering rate of electrons in a heterostructure is accurately given by assuming that the interface modes are pure interface vibrations at the LO frequency of the host material.²⁰ Both in the QW and in the free-standing wafer, mixing of interface and bulklike modes can be neglected, since the scattering is approximately invariant with respect to mixing of nearly degenerate modes. As noted above, the scattering by bulklike vibrations is the same in the two systems if the electrons are perfectly confined to the GaAs. Thus differences between the scattering properties of the semiconductor QW and of the free-standing wafer can be estimated by comparing the form factors for the interface vibrations.

Figure 7 illustrates the scattering form factors for the interface vibrations of both a GaAs/AlAs QW [with values of $\epsilon_1(\infty)$ and $\epsilon_2(\infty)$ given in Sec. VI D] and a free-standing GaAs wafer [with no barrier vibrations and $\epsilon_1(\infty)=1$]. The scattering by interface vibrations of the

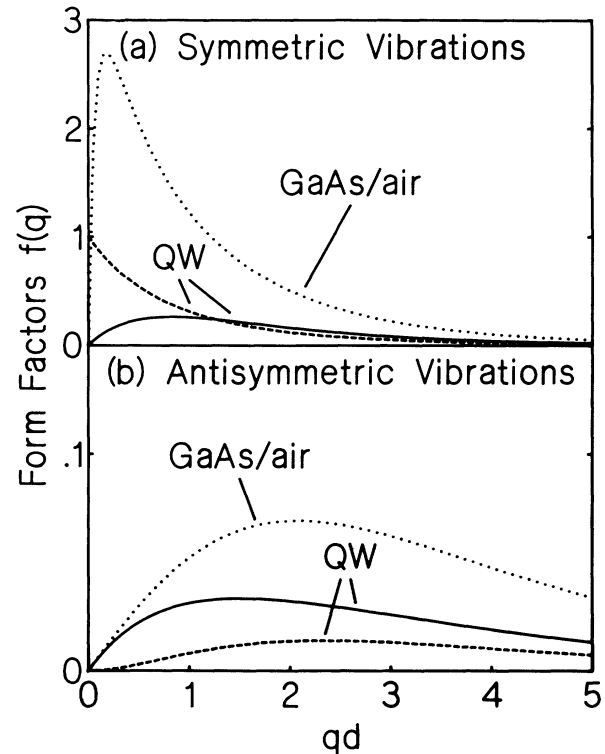


FIG. 7. Form factors for electron-phonon scattering by interface vibrations in a free-standing GaAs wafer (labeled GaAs/air) and in a GaAs/AlAs quantum well (labeled QW). The QW form factors are those for the interface vibrations of the well (solid curve) and of the barriers (dashed curve). The scattering of perfectly confined electrons (a) in the lowest subband (by symmetric vibrations), and (b) between the lowest two subbands (by antisymmetric vibrations), is considered.

GaAs layer is stronger if the layer is free standing than if it is clad by AlAs barriers. It is clear that this stronger scattering in the free-standing wafer outweighs the absence of scattering by interface vibrations of the barrier, except for symmetric vibrations with very small q (in the present example, with qd less than 0.02).

¹K. Hirakawa and H. Sakaki, Phys. Rev. B **33**, 8291 (1986).

²J. Shah, A. Pinczuk, A. C. Gossard, and W. Wiegmann, Phys. Rev. Lett. **54**, 2045 (1985).

³A. Seilmeier, H. J. Hübner, G. Abstreiter, G. Weimann, and W. Schlapp, Phys. Rev. Lett. **59**, 1345 (1987).

⁴M. C. Tatham, J. F. Ryan, and C. T. Foxon, Phys. Rev. Lett. **63**, 1637 (1989).

⁵D. A. B. Miller, D. S. Chemla, D. J. Eilenberger, P. W. Smith, A. C. Gossard, and W. T. Tsang, Appl. Phys. Lett. **41**, 679 (1982).

⁶T. Hiroshima, Solid State Commun. **68**, 483 (1988).

⁷K. J. Nash and D. J. Mowbray, J. Lumin. **44**, 315 (1989).

⁸E. Richter and D. Strauch, Solid State Commun. **64**, 867 (1987); S.-F. Ren, H. Chu, and Y.-C. Chang, Phys. Rev. Lett. **59**, 1841 (1987); Phys. Rev. B **37**, 8899 (1988); H. Chu, S.-F.

Ren, and Y.-C. Chang, *ibid.* B **37**, 10746 (1988); F. Bechstedt and H. Gerecke, Phys. Status Solidi B **154**, 565 (1989).

⁹A. K. Sood, J. Menendez, M. Cardona, and K. Ploog, Phys. Rev. Lett. **54**, 2111 (1985).

¹⁰R. Lassnig, Phys. Rev. B **30**, 7132 (1984).

¹¹K. Huang and B. Zhu, Phys. Rev. B **38**, 13377 (1988).

¹²S. Rudin and T. L. Reinecke, Phys. Rev. B **41**, 7713 (1990); **43**, 9298(E) (1991).

¹³B. K. Ridley, Phys. Rev. B **39**, 5282 (1989).

¹⁴M. Babiker, J. Phys. C **19**, 683 (1986).

¹⁵M. Babiker, M. P. Chamberlain, and B. K. Ridley, Semicond. Sci. Technol. **2**, 582 (1987).

¹⁶M. Babiker, J. Phys. C **19**, L339 (1986); M. Babiker and B. K. Ridley, Superlatt. Microstruct. **2**, 287 (1986); M. Babiker, M. P. Chamberlain, A. Ghosal, and B. K. Ridley, Surf. Sci. **196**,

- 422 (1988); M. Babiker, A. Ghosal, and B. K. Ridley, *Superlatt. Microstruct.* **5**, 133 (1989).
- ¹⁷M. V. Klein, *IEEE J. Quantum Electron.* **QE-22**, 1760 (1986).
- ¹⁸M. Cardona, *Superlatt. Microstruct.* **5**, 27 (1989).
- ¹⁹K. J. Nash, M. S. Skolnick, and S. J. Bass, *Semicond. Sci. Technol.* **2**, 329 (1987).
- ²⁰A. J. Read and K. J. Nash (unpublished).
- ²¹F. Bechstedt and H. Gerecke, *Phys. Status Solidi B* **156**, 151 (1989); *J. Phys. Condens. Matter* **2**, 4363 (1990).
- ²²T. Tsuchiya, H. Akera, and T. Ando, *Phys. Rev. B* **39**, 6025 (1989); H. Akera and T. Ando, *ibid.* **40**, 2914 (1989).
- ²³H. Gerecke and F. Bechstedt, *Phys. Rev. B* **43**, 7053 (1991).
- ²⁴See, for example, Z. V. Popović, M. Cardona, E. Richter, D. Strauch, L. Tapfer, and K. Ploog, *Phys. Rev. B* **41**, 5904 (1990).
- ²⁵H. Goldstein, *Classical Mechanics* (Addison-Wesley, New York, 1950).
- ²⁶Lord Rayleigh, *The Theory of Sound*, 2nd ed. (Dover, New York, 1945).
- ²⁷H. Margenau and G. M. Murphy, *The Mathematics of Physics and Chemistry*, 2nd ed. (Van Nostrand, Princeton, 1956).
- ²⁸D. Strauch and B. Dorner, *J. Phys. Condens. Matter* **2**, 1457 (1990).
- ²⁹The labels TE and TM will be used although, in the present electrostatic theory, the electromagnetic fields associated with bulklike TO vibrations are neglected. The TE vibrations have $w_y \neq 0$, $w_x = w_z = 0$, and the TM vibrations have $w_x, w_z \neq 0$, $w_y = 0$.
- ³⁰R. E. Fern and A. Onton, *J. Appl. Phys.* **42**, 3499 (1971).
- ³¹A. Onton, in *Proceedings of the 10th International Conference on the Physics of Semiconductors, Cambridge, MA, 1970*, edited by S. P. Keller, J. C. Hensel, and F. Stern (United States Atomic Energy Commission Division of Technical Information, Oak Ridge, TN, 1970), p. 107.
- ³²G. A. Samara, *Phys. Rev. B* **27**, 3494 (1983).
- ³³O. K. Kim and W. G. Spitzer, *J. Appl. Phys.* **50**, 4362 (1979).
- ³⁴J. E. Zucker, A. Pinczuk, D. S. Chemla, A. Gossard, and W. Wiegmann, *Phys. Rev. Lett.* **53**, 1280 (1984) achieved this by performing right-angle Raman scattering on a superlattice in a waveguide structure.
- ³⁵B. K. Ridley and M. Babiker, *Phys. Rev. B* **43**, 9096 (1991).
- ³⁶B. K. Ridley, *Phys. Rev. B* **44**, 9002 (1991).
- ³⁷It is interesting to note that state-of-the-art Raman-scattering studies (Ref. 24) often compare experimental results directly with microscopic calculations rather than continuum models.
- ³⁸In addition, neglect of the finite cutoff on the number of polar-optic branches, $n \lesssim N$, will not lead to significant errors in scattering rates.
- ³⁹J. K. Jain and S. Das Sarma, *Phys. Rev. Lett.* **62**, 2305 (1989).
- ⁴⁰B. K. Ridley, *Semicond. Sci. Technol.* **4**, 1142 (1989). Section 6 of this paper argues that in the hot-phonon regime, the relaxation of carrier momentum is stronger when the normal modes are modified by well-width fluctuations and other disorder than it is for phonons with Bloch symmetry, since one of the latter contributes no overall loss of momentum when it is created and then destroyed by electron-phonon interactions. (Note that the QW scattering rates in this paper are calculated using the theory of Refs. 14–16.)
- ⁴¹N. C. Constantinou and B. K. Ridley, *J. Phys. Condens. Matter* **2**, 7465 (1990).
- ⁴²Reference 27, Chap. 8.